Come with rain, O loud Southwester!
Bring the singer, bring the nester;
Give the buried flower a dream;
Make the settled snowbank steam.
Robert Frost, *To the Thawing Wind*, 1915.

CHAPTER 9

Barotropic and Baroclinic Instability

WHAT HYDRODYNAMIC STATES OCCUR IN NATURE? If we take as given the applicability of the Navier–Stokes equations, any flow must be a solution of these equations, subject to the relevant initial and boundary conditions. Most of the flows we experience are of course *time-dependent* solutions, not steady solutions. Why should this be? There are many steady solutions to the equations of motion — certain purely zonal flows, for example. However, steady solutions do not abound in nature because, in order to persist, they must be stable to those small perturbations that inevitably arise. Indeed, all the steady solutions that are known for the large-scale flow in the Earth's atmosphere and ocean have been found to be unstable. It is such instability that makes the subject an interesting one.

There are a myriad forms of hydrodynamic instability, but our focus in this chapter is on barotropic and baroclinic instability. *Baroclinic instability* (and we will define the term more precisely later on) is an instability that arises in rotating, stratified fluids that are subject to a horizontal temperature gradient. It is the instability that gives rise to the large- and mesoscale motion in the atmosphere and ocean — it produces atmospheric weather systems, for example — and so is, perhaps, the form of hydrodynamic instability that most affects the human condition. *Barotropic instability* is an instability that arises because of the shear in a flow, and may occur in fluids of constant density. It is important to us for two reasons: first, it is important in its own right as an instability mechanisms for jets and vortices, and as an important process in both two- and three-dimensional turbulence; second, many problems in barotropic and baroclinic instability are formally and dynamically similar, so that the solutions and insight we obtain in the often simpler problems in barotropic instability may be useful in the baroclinic problem.

9.1 KELVIN–HELMHOLTZ INSTABILITY

To introduce the issue, we first consider, rather informally, perhaps the simplest physically interesting instance of a fluid-dynamical instability — that of a constant-density flow with a shear perpendicular to the fluid's mean velocity, this being an example of a *Kelvin–Helmholtz instability,*[1] and of a barotropic instability. (More generally, Kelvin–Helmholtz instability involves fluid with varying density.) Let us consider two fluid masses of equal density, with a common interface at $y = 0$, moving with velocities $-U$ and $+U$ in the x-direction, respectively (Fig. 9.1). There is no variation in the basic flow in the z-direction (normal to the page), and we will assume this is also true for the instability (these restrictions are not essential). This flow is clearly a solution of

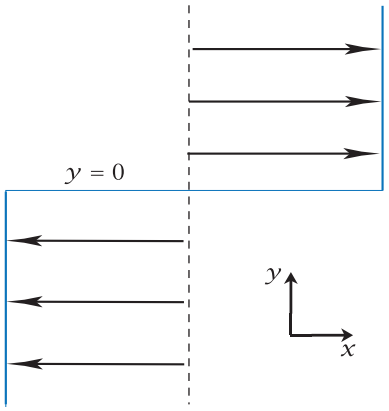

Fig. 9.1 A simple basic state giving rise to shear-flow instability. The velocity profile is discontinuous and the density is uniform.

the Euler equations. What happens if the flow is perturbed slightly? If the perturbation is initially small then even if it grows we can, for small times after the onset of instability, neglect the nonlinear interactions in the governing equations because these are the squares of small quantities. The equations determining the evolution of the initial perturbation are then the Euler equations linearized about the steady solution. Thus, denoting perturbation quantities with a prime and basic state variables with capital letters, for $y > 0$ the perturbation satisfies

$$\frac{\partial \boldsymbol{u}'}{\partial t} + U\frac{\partial \boldsymbol{u}'}{\partial x} = -\nabla p', \qquad \nabla \cdot \boldsymbol{u}' = 0, \tag{9.1a,b}$$

and a similar equation holds for $y < 0$, but with U replaced by $-U$. Given periodic boundary conditions in the x-direction, we may seek solutions of the form

$$\phi'(x, y, t) = \mathrm{Re} \sum_k \tilde{\phi}_k(y) \exp[\mathrm{i}k(x - ct)], \tag{9.2}$$

where ϕ is any field variable (e.g., pressure or velocity), and Re denotes that only the real part should be taken. (Typically we use tildes over variables to denote Fourier-like modes, and we will often omit the marker 'Re'.) Because (9.1a) is linear, the Fourier modes do not interact and we may confine attention to just one. Taking the divergence of (9.1a), the left-hand side vanishes and the pressure satisfies Laplace's equation

$$\nabla^2 p' = 0. \tag{9.3}$$

This has solutions in the form

$$p' = \begin{cases} \mathrm{Re}\, \tilde{p}_1 \mathrm{e}^{\mathrm{i}kx - ky} \mathrm{e}^{\sigma t} & y > 0, \\ \mathrm{Re}\, \tilde{p}_2 \mathrm{e}^{\mathrm{i}kx + ky} \mathrm{e}^{\sigma t} & y < 0, \end{cases} \tag{9.4}$$

where, anticipating the possibility of growing solutions, we have written the time variation in terms of a growth rate, $\sigma = -\mathrm{i}kc$. In general σ is complex: if it has a positive real component, the amplitude of the perturbation will grow and there is an instability; if σ has a non-zero imaginary component, then there will be oscillatory motion, and there may be both oscillatory motion *and* an instability. To obtain the dispersion relationship, we consider the y-component of (9.1a), namely (for $y > 0$)

$$\frac{\partial v_1'}{\partial t} + U\frac{\partial v_1'}{\partial x} = -\frac{\partial p_1'}{\partial y}. \tag{9.5}$$

Substituting a solution of the form $v_1' = \tilde{v}_1 \exp(\mathrm{i}kx + \sigma t)$ yields, with (9.4),

$$(\sigma + \mathrm{i}kU)\tilde{v}_1 = k\tilde{p}_1. \tag{9.6}$$

But the velocity normal to the interface is, at the interface, nothing but the rate of change of the position of the interface itself; that is, at $y = +0$

$$v_1 = \frac{\partial \eta'}{\partial t} + U\frac{\partial \eta'}{\partial x}, \tag{9.7}$$

or

$$\tilde{v}_1 = (\sigma + \mathrm{i}kU)\tilde{\eta}, \tag{9.8}$$

where η' is the displacement of the interface from its equilibrium position. Using this in (9.6) gives

$$(\sigma + \mathrm{i}kU)^2\tilde{\eta} = k\tilde{p}_1. \tag{9.9}$$

The above few equations pertain to motion on the $y > 0$ side of the interface. Similar reasoning on the other side gives (at $y = -0$)

$$(\sigma - \mathrm{i}kU)^2\tilde{\eta} = -k\tilde{p}_2. \tag{9.10}$$

But at the interface $p_1 = p_2$, because pressure must be continuous. The dispersion relationship then emerges from (9.9) and (9.10), giving

$$\sigma^2 = k^2U^2. \tag{9.11}$$

This equation has two roots, one of which is positive. Thus, the amplitude of the perturbation grows exponentially, like $\mathrm{e}^{\sigma t}$, and the flow is *unstable*. The instability itself can be seen in the natural world when billow clouds appear wrapped up into spirals: the clouds are acting as tracers of fluid flow, and are a manifestation of the instability at finite amplitude, as seen later in Fig. 9.6.

9.2 INSTABILITY OF PARALLEL SHEAR FLOW

We now consider a little more systematically the instability of *parallel shear flows,* such as are illustrated in Fig. 9.2. This is a classic problem in hydrodynamic stability theory, and there are two particular reasons for our own interest:

(i) The instability is an example of *barotropic instability,* which abounds in the ocean and atmosphere. Roughly speaking, barotropic instability arises when a flow is unstable by virtue of its horizontal shear, with gravitational and buoyancy effects being secondary.

(ii) The instability is in many ways analogous to *baroclinic instability,* which is the main instability giving rise to weather systems in the atmosphere and similar phenomena in the ocean.

We will restrict attention to two-dimensional, incompressible flow; this illustrates the physical mechanisms in the most transparent way, in part because it allows for the introduction of a streamfunction and the automatic satisfaction of the mass continuity equation. In fact, for parallel two-dimensional shear flows the most unstable disturbances are two-dimensional ones.[2]

The vorticity equation for incompressible two-dimensional flow is just

$$\frac{\mathrm{D}\zeta}{\mathrm{D}t} = 0. \tag{9.12}$$

We suppose the basic state to be a parallel flow in the x-direction that may vary in the y-direction. That is

$$\overline{\boldsymbol{u}} = U(y)\mathbf{i}. \tag{9.13}$$

The linearized vorticity equation is then

$$\frac{\partial \zeta'}{\partial t} + U\frac{\partial \zeta'}{\partial x} + v'\frac{\partial \mathcal{Z}}{\partial y} = 0, \tag{9.14}$$

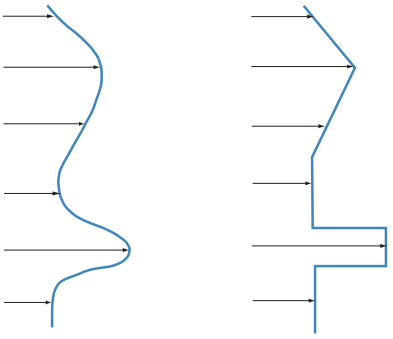

Fig. 9.2 Left: example of a smooth velocity profile, in which both the velocity and the vorticity are continuous. Right: example of a piecewise continuous profile, in which the velocity and vorticity may have finite discontinuities.

where $\mathcal{Z} = -\partial_y U$. Because the mass continuity equation has the simple form $\partial u'/\partial x + \partial v'/\partial y = 0$, we may introduce a streamfunction ψ such that $u' = -\partial\psi'/\partial y$, $v' = \partial\psi'/\partial x$ and $\zeta' = \nabla^2\psi'$. The linear vorticity equation becomes

$$\frac{\partial\nabla^2\psi'}{\partial t} + U\frac{\partial\nabla^2\psi'}{\partial x} + \frac{\partial\mathcal{Z}}{\partial y}\frac{\partial\psi'}{\partial x} = 0. \tag{9.15}$$

The coefficients of the x-derivatives are not themselves functions of x; thus, we may seek solutions that are harmonic functions (sines and cosines) in the x-direction, but the y dependence must remain arbitrary at this stage and we write

$$\psi' = \mathrm{Re}\,\tilde{\psi}(y)\mathrm{e}^{\mathrm{i}k(x-ct)}. \tag{9.16}$$

The full solution is a superposition of all wavenumbers, but since the problem is linear the waves do not interact and it suffices to consider them separately. If c is purely real then c is the phase speed of the wave; if c has a positive imaginary component then the wave will grow exponentially and is thus *unstable*.

From (9.16) we have

$$u' = \tilde{u}(y)\mathrm{e}^{\mathrm{i}k(x-ct)} = -\tilde{\psi}_y\mathrm{e}^{\mathrm{i}k(x-ct)}, \tag{9.17a}$$

$$v' = \tilde{v}(y)\mathrm{e}^{\mathrm{i}k(x-ct)} = \mathrm{i}k\tilde{\psi}\mathrm{e}^{\mathrm{i}k(x-ct)}, \tag{9.17b}$$

$$\zeta' = \tilde{\zeta}(y)\mathrm{e}^{\mathrm{i}k(x-ct)} = (-k^2\tilde{\psi} + \tilde{\psi}_{yy})\mathrm{e}^{\mathrm{i}k(x-ct)}, \tag{9.17c}$$

where the y subscript denotes a derivative. Using (9.17) in (9.14) gives

$$(U-c)(\tilde{\psi}_{yy} - k^2\tilde{\psi}) - U_{yy}\tilde{\psi} = 0, \tag{9.18}$$

which is known as *Rayleigh's equation*.[3] It is the linear vorticity equation for disturbances to parallel shear flow, and in the presence of a β-effect it generalizes slightly to

$$(U-c)(\tilde{\psi}_{yy} - k^2\tilde{\psi}) + (\beta - U_{yy})\tilde{\psi} = 0, \tag{9.19}$$

which is known as the Rayleigh–Kuo equation.

9.2.1 Piecewise Linear Flows

Although Rayleigh's equation is linear and has a simple form, it is nevertheless quite difficult to analytically solve for an arbitrary smoothly varying profile. It is simpler to consider *piecewise linear*

flows, in which U_y is a constant over some interval, with U or U_y changing abruptly to another value at a line of discontinuity, as illustrated in Fig. 9.2. The curvature, U_{yy} is accounted for through the satisfaction of matching conditions, analogous to boundary conditions, at the lines of discontinuity (as in Section 9.1), and solutions in each interval are then exponential functions.

Jump or matching conditions

The idea, then, is to solve the linearized vorticity equation separately in the continuous intervals in which vorticity is constant, matching the solution with that in the adjacent regions. The matching conditions arise from two physical conditions:

(i) That normal stress should be continuous across the interface. For an inviscid fluid this implies that pressure be continuous.

(ii) That the normal velocity of the fluid on either side of the interface should be consistent with the motion of the interface itself.

Let us consider the implications of these two conditions.

(i) Continuity of pressure

The linearized momentum equation in the direction along the interface is:

$$\frac{\partial u'}{\partial t} + U\frac{\partial u'}{\partial x} + v'\frac{\partial U}{\partial y} = -\frac{\partial p'}{\partial x}. \tag{9.20}$$

For normal modes, $u' = -\tilde{\psi}_y e^{ik(x-ct)}$, $v' = ik\tilde{\psi}e^{ik(x-ct)}$ and $p' = \tilde{p}e^{ik(x-ct)}$, and (9.20) becomes

$$ik(U-c)\tilde{\psi}_y - ik\tilde{\psi}U_y = -ik\tilde{p}. \tag{9.21}$$

Because pressure is continuous across the interface we have the first *matching* or *jump condition,*

$$\Delta[(U-c)\tilde{\psi}_y - \tilde{\psi}U_y] = 0, \tag{9.22}$$

where the operator Δ denotes the difference in the values of the argument (in square brackets) across the interface. That is, the quantity $(U-c)\tilde{\psi}_y - \tilde{\psi}U_y$ is continuous.

We can obtain this condition directly from Rayleigh's equation, (9.19), written in the form

$$[(U-c)\tilde{\psi}_y - U_y\tilde{\psi}]_y + [\beta - k^2(U-c)]\tilde{\psi} = 0. \tag{9.23}$$

Integrating across the interface gives (9.22).

(ii) Material interface condition

At the interface, the normal velocity v is given by the kinematic condition

$$v = \frac{D\eta}{Dt}, \tag{9.24}$$

where η is the interface displacement. The linear version of (9.24) is

$$\frac{\partial \eta'}{\partial t} + U\frac{\partial \eta'}{\partial x} = \frac{\partial \psi'}{\partial x}. \tag{9.25}$$

If the fluid itself is continuous then this equation must hold at either side of the interface, giving two equations and their normal-mode counterparts, namely,

$$\frac{\partial \eta'}{\partial t} + U_1\frac{\partial \eta'}{\partial x} = \frac{\partial \psi_1'}{\partial x} \quad \longrightarrow \quad (U_1 - c)\tilde{\eta} = \tilde{\psi}_1, \tag{9.26}$$

$$\frac{\partial \eta'}{\partial t} + U_2 \frac{\partial \eta'}{\partial x} = \frac{\partial \psi_2'}{\partial x} \quad \longrightarrow \quad (U_2 - c)\tilde{\eta} = \tilde{\psi}_2. \tag{9.27}$$

Material continuity at the interface thus gives the second jump condition

$$\Delta\left[\frac{\tilde{\psi}}{U-c}\right] = 0. \tag{9.28}$$

That is, $\tilde{\psi}/(U-c)$ is continuous at the interface. Note that if U is continuous across the interface the condition becomes one of continuity of the normal velocity.

9.2.2 Kelvin–Helmholtz Instability, Revisited

We now use Rayleigh's equation and the jump conditions to consider the situation illustrated in Fig. 9.1; that is, vorticity is everywhere zero except in a thin sheet at $y = 0$. On either side of the interface, Rayleigh's equation is simply

$$(U_i - c)(\partial_{yy}\tilde{\psi}_i - k^2\tilde{\psi}_i) = 0, \qquad i = 1, 2 \tag{9.29}$$

or, assuming that $U_i \neq c$, $\partial_{yy}\tilde{\psi}_i - k^2\tilde{\psi}_i = 0$. (This is just Laplace's equation, coming from $\nabla^2\psi' = \zeta'$, with $\zeta' = 0$ everywhere except at the interface.) Solutions of this that decay away on either side of the interface are

$$y > 0: \qquad \tilde{\psi}_1 = \Psi_1 \mathrm{e}^{-ky}, \tag{9.30a}$$

$$y < 0: \qquad \tilde{\psi}_2 = \Psi_2 \mathrm{e}^{ky}, \tag{9.30b}$$

where Ψ_1 and Ψ_2 are constants. The boundary condition (9.22) gives

$$(U_1 - c)(-k)\Psi_1 = (U_2 - c)(k)\Psi_2, \tag{9.31}$$

and (9.28) gives

$$\frac{\Psi_1}{(U_1 - c)} = \frac{\Psi_2}{(U_2 - c)}. \tag{9.32}$$

The last two equations combine to give $(U_1 - c)^2 = -(U_2 - c)^2$, which, supposing that $U = U_1 = -U_2$ gives $c^2 = -U^2$. Thus, since U is purely real, $c = \pm \mathrm{i}U$, and the disturbance grows exponentially as $\exp(kU_1 t)$, just as we obtained in Section 9.1. All wavelengths are unstable, and indeed the shorter the wavelength the greater the instability. In reality, viscosity will damp the smallest waves, although the presence of viscosity would also mean that the initial profile is not an exact, steady solution of the equations of motion.

9.2.3 Edge Waves

We now consider a case sketched in Fig. 9.3 in which the velocity is continuous, but the vorticity is discontinuous. Since on either side of the interface $U_{yy} = 0$, Rayleigh's equation is just

$$(U(y) - c)(\tilde{\psi}_{yy} - k^2\tilde{\psi}) = 0. \tag{9.33}$$

Provided $c \neq U$ this has solutions,

$$\tilde{\psi} = \begin{cases} \Phi_1 \mathrm{e}^{-ky} & y > 0 \\ \Phi_2 \mathrm{e}^{ky} & y < 0. \end{cases} \tag{9.34}$$

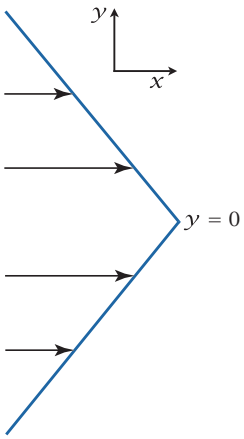

Fig. 9.3 Velocity profile of a point jet, in which vorticity is concentrated at a point. Although the vorticity is discontinuous, a small perturbation gives rise only to *edge waves* centred at $y = 0$, and so the jet is stable.

The value of c is found by applying the jump conditions (9.22) and (9.28) at $y = 0$. Using (9.34) these give

$$-k(U_0 - c)\Phi_1 - \Phi_1 \partial_y U_1 = k(U_0 - c)\Phi_2 - \Phi_2 \partial_y U_2 \tag{9.35a}$$

$$\Phi_1 = \Phi_2, \tag{9.35b}$$

where $U_1(y)$ and $U_2(y)$ are the velocities on either side of the interface, and both are equal to U_0 at the interface. (In Fig. 9.3 we illustrate the case with $U_1 = -Ay$ and $U_2 = Ay$, where A is a positive constant.) After a line of algebra the above equations give

$$c = U_0 + \frac{\partial_y U_1 - \partial_y U_2}{2k}. \tag{9.36}$$

This is the dispersion relationship for *edge waves* that propagate along the interface with speed equal to the sum of the fluid speed and a factor proportional to the difference in the vorticity between the two layers. No matter what the shear is on either side of the interface, the phase speed is purely real and there is no instability. Equation (9.36) is analogous to the Rossby wave dispersion relation $c = U_0 - \beta/K^2$, and reflects a similarity in the physics — β is a planetary vorticity gradient, which in (9.36) is collapsed to a front and represented by the difference $\partial_y U_1 - \partial_y U_2 = -(\mathcal{Z}_1 - \mathcal{Z}_2)$, where $\mathcal{Z}_1$ and $\mathcal{Z}_2$ are the basic-state vorticities on either side of the interface. One might even say that such edge waves *are* Rossby waves of a very simple form.

9.2.4 Interacting Edge Waves Producing Instability

Now we consider a slightly more complicated case in which edge waves may interact giving rise, as we shall see, to an instability. The physical situation is illustrated in Fig. 9.4. We consider the simplest case, that of a shear layer (which we denote as region 2) sandwiched between two semi-infinite layers, regions 1 and 3, as in the left-hand panel of the figure. Thus, the basic state is

$$y > a: \qquad U = U_1 = U_0 \ \text{(a constant)}, \tag{9.37a}$$

$$-a < y < a: \qquad U = U_2 = \frac{U_0}{a} y, \tag{9.37b}$$

$$y < -a: \qquad U = U_3 = -U_0. \tag{9.37c}$$

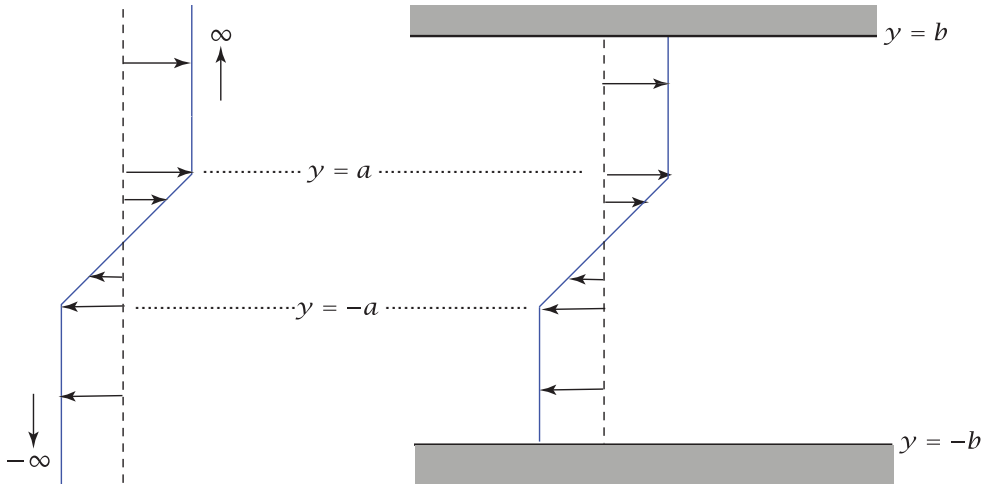

Fig. 9.4 Barotropically unstable velocity profiles. In the simplest case, on the left, a region of shear is sandwiched between two infinite regions of constant velocity. The edge waves at $y = \pm a$ interact to produce an instability. If $a = 0$, then the situation corresponds to that of Fig. 9.1, giving Kelvin–Helmholtz instability. In the case on the right, the flow is bounded at $y = \pm b$. The flow is unstable provided that b is sufficiently larger than a. If $b = a$ (plane Couette flow) the flow is stable to infinitesimal disturbances.

We assume a solution of Rayleigh's equation of the form:

$$y > a: \qquad \tilde{\psi}_1 = A\mathrm{e}^{-k(y-a)}, \tag{9.38a}$$

$$-a < y < a: \qquad \tilde{\psi}_2 = B\mathrm{e}^{k(y-a)} + C\mathrm{e}^{-k(y+a)}, \tag{9.38b}$$

$$y < -a: \qquad \tilde{\psi}_3 = D\mathrm{e}^{k(y+a)}. \tag{9.38c}$$

These particular forms all decay away from the interfaces at the edges of domains in which the assumed solutions apply, as edge waves must do. Applying the jump conditions (9.22) and (9.28) at the interfaces at $y = a$ and $y = -a$ gives the following relations between the coefficients:

$$-A[(U_0 - c)k] = B\left[(U_0 - c)k - \frac{U_0}{a}\right] - C\mathrm{e}^{-2ka}\left[\frac{U_0}{a} + (U_0 - c)k\right], \tag{9.39a}$$

$$A = B + C\mathrm{e}^{-2ka}, \tag{9.39b}$$

$$D[(U_0 + c)k] = B\mathrm{e}^{-2ka}\left[(U_0 + c)k + \frac{U_0}{a}\right] + C\left[\frac{U_0}{a} - (U_0 + c)k\right], \tag{9.39c}$$

$$D = B\mathrm{e}^{-2ka} + C. \tag{9.39d}$$

These are a set of four homogeneous equations, with the unknown parameters A, B, C and D, which may be written in the form of a matrix equation,

$$\begin{pmatrix} k(U_0 - c) & k(U_0 - c) - U_0/a & -\mathrm{e}^{-2ka}[U_0/a + k(U_0 - c)] & 0 \\ 1 & -1 & -\mathrm{e}^{-2ka} & 0 \\ 0 & -\mathrm{e}^{-2ka}[k(U_0 + c) + U_0/a] & k(U_0 + c) - (U_0/a) & k(U_0 + c) \\ 0 & \mathrm{e}^{-2ka} & 1 & -1 \end{pmatrix} \begin{pmatrix} A \\ B \\ C \\ D \end{pmatrix} = 0. \tag{9.40}$$

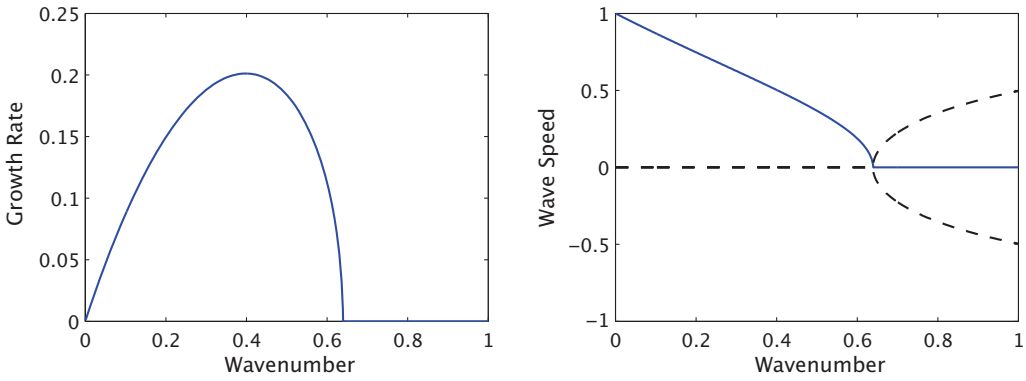

Fig. 9.5 Left: Growth rate ($\sigma = kc_i$) calculated from (9.41) with c nondimensionalized by U_0 and k nondimensionalized by $1/a$ (equivalent to setting $a = U_0 = 1$). Right: Real (c_r, dashed) and imaginary (c_i, solid) wave speeds. The flow is unstable for $k < 0.63$, with the maximum instability occurring at $k = 0.39$.

For non-trivial solutions the determinant of the matrix must be zero, and solving the ensuing equation gives, after some algebra, the dispersion relationship[4]

$$c^2 = \left(\frac{U_0}{2ka}\right)^2 \left[(1-2ka)^2 - \mathrm{e}^{-4ka}\right], \tag{9.41}$$

and this is plotted in Fig. 9.5. The flow is unstable for sufficiently long wavelengths, since then the right-hand side of (9.41) is negative. The critical wavenumber below which instability occurs is found by solving $(1-2ka)^2 = \mathrm{e}^{-4ka}$, which gives instability for $ka < 0.63293$. A numerical solution of the initial value problem is illustrated in Figs. 9.6 and 9.7. Here, the initial perturbation is small and random, containing components at all wavenumbers. All the modes in the unstable range grow exponentially, and the pattern is soon dominated by the mode that grows fastest — a horizontal wavenumber of 3 in this problem. Eventually, the perturbation grows sufficiently that the linear equations are no longer valid and, as is seen in the second column of Fig. 9.6, vortices form and pinch off. The vortices interact and the flow develops into two-dimensional turbulence, as considered in Chapter 11.

The mechanism of the instability — an informal view

(A similar mechanism is discussed in Section 9.7, and the reader may wish to read the two descriptions in tandem.) We have seen that an edge wave in isolation is stable, with the instability arising when two edge waves have sufficient cross-stream extent that they can interact with each other. This occurs for sufficiently long wavelengths because the cross-stream decay scale is proportional to the along-stream wavelength — hence the high-wavenumber cut-off. To see the mechanism of the instability transparently, let us first suppose that the interfaces are, in fact, sufficiently far away that the edge waves at each interface do not interact. Using (9.36) the edge waves at $y = -a$ and $y = +a$ have dispersion relationships

$$c_{+a} = U_0 - \frac{U_0/a}{2k}, \qquad c_{-a} = -U_0 + \frac{U_0/a}{2k}. \tag{9.42a,b}$$

If the two waves are to interact these phase speeds must be equal, giving the condition

$$c = 0, \qquad k = 1/(2a). \tag{9.43a,b}$$

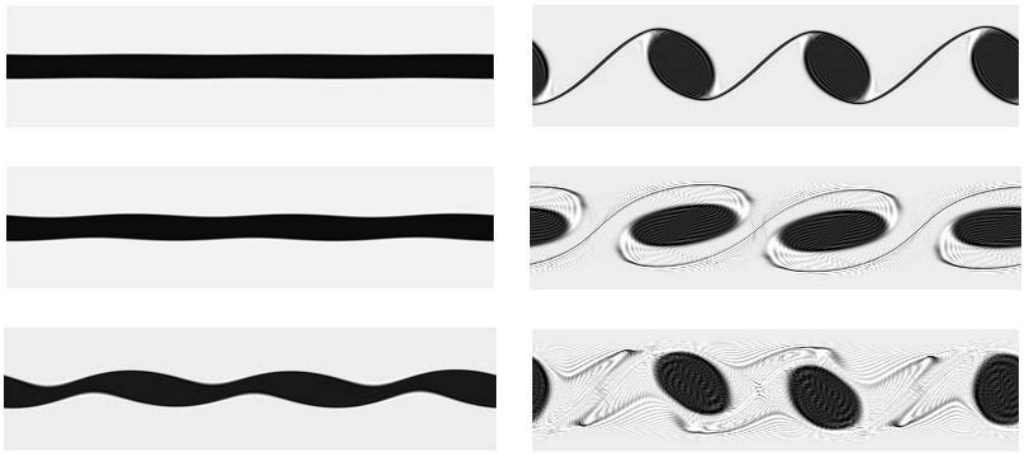

Fig. 9.6 A sequence of plots of the vorticity, at equal time intervals, from a numerical solution of the nonlinear vorticity equation (9.12), with initial conditions as in Fig. 9.4 with $a = 0.1$, plus a very small random perturbation. Time increases first down the left column and then down the right column. The solution is obtained in a rectangular (4×1) domain, with periodic conditions in the x-direction and slippery walls at $y = (0, 1)$. The maximum linear instability occurs for a wavelength of 1.57, which for a domain of length 4 corresponds to a wavenumber of 2.55. Since the periodic domain quantizes the allowable wavenumbers, the maximum instability is at wavenumber 3, and this is what emerges. Only in the first two or three frames is the linear approximation valid.

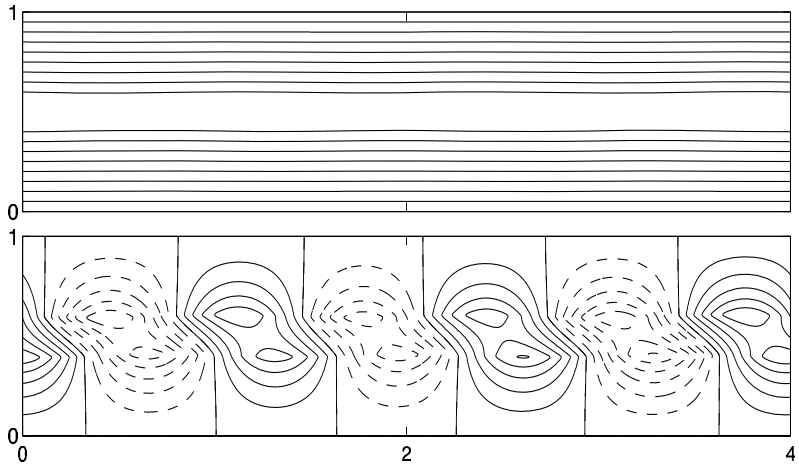

Fig. 9.7 The total streamfunction (top panel) and the perturbation streamfunction from the same numerical calculation as in Fig. 9.6, at a time corresponding to the second frame. Positive values are solid lines, and negative values are dashed. The perturbation pattern leans into the shear, and grows exponentially in place.

That is, the waves are stationary, and their wavelength is proportional to the separation of the two edges. In fact, (9.43) approximately characterizes the conditions at the critical wavenumber $k = 0.63/a$ (see Fig. 9.5). In the region of the shear the two waves have the form

$$\psi_{+a} = \mathrm{Re}\,\tilde{\psi}_{+a}(t)\mathrm{e}^{k(y-a)}\mathrm{e}^{\mathrm{i}\phi}\mathrm{e}^{\mathrm{i}kx}, \qquad \psi_{-a} = \mathrm{Re}\,\tilde{\psi}_{-a}(t)\mathrm{e}^{-k(y+a)}\mathrm{e}^{\mathrm{i}kx}, \tag{9.44a,b}$$

where ϕ is the phase shift between the waves; in the case of pure edge waves we have $\tilde{\psi}_{\pm a} = A_{\pm a}\mathrm{e}^{-\mathrm{i}kct}$ where we may take $A_{\pm a}$ to be real.

Now consider how the wave generated at $y = -a$ might affect the wave at $y = +a$ and vice versa. The contribution of ψ_{-a} to the acceleration of ψ_{+a} is given by applying the x-momentum equation, (9.20), at $y = +a$. Thus we take the kinematic solutions, (9.44), and use them in a dynamical equation, the momentum equation, to calculate the ensuing acceleration. At $y = +a$ we heuristically write

$$\frac{\partial u'_{+a}}{\partial t} = -[v'_{+a}(+a) + v'_{-a}(+a)]\frac{\mathrm{d}U}{\mathrm{d}y} \tag{9.45}$$

with a similar expression at $y = -a$, and omitting the pressure terms. Here $v'_{-a}(+a)$ denotes the value of v at $y = +a$ due to the edge wave generated at $-a$. It is the second term on the right-hand side that is necessary for any potential instability, as the first term gives only neutral edge waves. If the spatial dependence of the waves is given by (9.44), then at $y = +a$ we have, omitting the contribution from the edge waves,

$$\frac{\partial u'_{+a}}{\partial t} = -v'_{-a}(+a)\frac{\mathrm{d}U}{\mathrm{d}y} \qquad \Rightarrow \qquad -k\mathrm{e}^{\mathrm{i}\phi}\mathrm{e}^{\mathrm{i}kx}\frac{\mathrm{d}\tilde{\psi}_{+a}}{\mathrm{d}t} = -\mathrm{i}k\mathrm{e}^{ikx}\mathrm{e}^{-2ka}\frac{\partial U}{\partial y}\tilde{\psi}_{-a}. \tag{9.46}$$

The real part of this equation is: $\cos(kx + \phi)\mathrm{d}\tilde{\psi}_{+a}/\mathrm{d}t = -\sin kx\,\mathrm{e}^{-2ka}\mathrm{d}U/\mathrm{d}y$. If the edge waves have the appropriate phase with respect to each other then the two edge waves can feed back on each other and couple to form a single growing mode. In particular if $\phi = \pi/2$ then the evolution equations for ψ_{+a} and ψ_{-a} become

$$\frac{\mathrm{d}\tilde{\psi}_{+a}}{\mathrm{d}t} = \mathrm{e}^{-2ka}\frac{\mathrm{d}U}{\mathrm{d}y}\tilde{\psi}_{-a}, \qquad \frac{\mathrm{d}\tilde{\psi}_{-a}}{\mathrm{d}t} = \mathrm{e}^{-2ka}\frac{\mathrm{d}U}{\mathrm{d}y}\tilde{\psi}_{+a}, \tag{9.47a,b}$$

which give exponential growth. When $\phi = \pi/2$ the wave at $y = +a$ lags the wave at $y = -a$, and *the unstable perturbation tilts into the shear;* this property of the instability is seen in the full solution, Fig. 9.7.

9.3 NECESSARY CONDITIONS FOR INSTABILITY

9.3.1 Rayleigh's Criterion

For simple profiles it may be possible to calculate, or even intuit, the instability properties, but for continuous profiles of $U(y)$ this is often impossible and it would be nice to have some general guidelines as to when a profile might be unstable. To this end, we derive a couple of *necessary* conditions for instability, or *sufficient* conditions for stability, that will at least tell us if a flow *might* be unstable. We begin by writing Rayleigh's equation, (9.19), as

$$\tilde{\psi}_{yy} - k^2\tilde{\psi} + \frac{\beta - U_{yy}}{U - c}\tilde{\psi} = 0. \tag{9.48}$$

Multiply by $\tilde{\psi}^*$ (the complex conjugate of $\tilde{\psi}$) and integrate over the domain of interest. After integrating the first term by parts we obtain

$$\int_{y_1}^{y_2}\left(\left|\frac{\partial\tilde{\psi}}{\partial y}\right|^2 + k^2|\tilde{\psi}|^2\right)\mathrm{d}y - \int_{y_1}^{y_2}\frac{\beta - U_{yy}}{U - c}|\tilde{\psi}|^2\,\mathrm{d}y = 0, \tag{9.49}$$

assuming that $\tilde{\psi}$ vanishes at the boundaries. (The limits to the integral may be infinite, in which case it is assumed that $\tilde{\psi}$ decays to zero as $|y|$ approaches ∞.) The only variable in this expression that is complex is c, and thus the first integral is real. The imaginary component of the second integral is

$$c_i \int \frac{\beta - U_{yy}}{|U-c|^2} |\tilde{\psi}|^2 \, \mathrm{d}y = 0. \tag{9.50}$$

Thus, *either* c_i vanishes or the integral does. For there to be an instability c_i must be non-zero. The eigenvalues of Rayleigh's equation come in pairs, for each decaying mode (negative c_i) there is a corresponding growing mode (positive c_i). If c_i is to be non-zero, the integrand of (9.50) must be zero and therefore:

A necessary condition for instability is that the expression

$$\beta - U_{yy}$$

change sign somewhere in the domain.

Equivalently, a sufficient criterion for stability is that $\beta - U_{yy}$ does not vanish in the domain interior. This condition is known as Rayleigh's inflection-point criterion, or when $\beta \neq 0$, the Rayleigh–Kuo inflection point criterion.[5]

A more general derivation

Consider again the vorticity equation, linearized about a parallel shear flow (cf. (9.14) with a β-term),

$$\frac{\partial \zeta}{\partial t} + U\frac{\partial \zeta}{\partial x} + v\left(\frac{\partial \mathcal{Z}}{\partial y} + \beta\right) = 0, \tag{9.51}$$

(dropping the primes on the perturbation quantities). Multiply by ζ and divide by $\beta + \mathcal{Z}_y$ to obtain

$$\frac{\partial}{\partial t}\left(\frac{\zeta^2}{\beta + \mathcal{Z}_y}\right) + \frac{U}{\beta + \mathcal{Z}_y}\frac{\partial \zeta^2}{\partial x} + 2v\zeta = 0, \tag{9.52}$$

and then integrate with respect to x to give

$$\frac{\partial}{\partial t}\int \left(\frac{\zeta^2}{\beta + \mathcal{Z}_y}\right) \mathrm{d}x = -2\int v\zeta \, \mathrm{d}x. \tag{9.53}$$

Now, using $\nabla \cdot \boldsymbol{u} = 0$, the vorticity flux may be written as

$$v\zeta = -\frac{\partial}{\partial y}(uv) + \frac{1}{2}\frac{\partial}{\partial x}(v^2 - u^2). \tag{9.54}$$

That is, *the flux of vorticity is the divergence of some quantity.* Its integral therefore vanishes provided there are no contributions from the boundary, and integrating (9.53) with respect to y gives

$$\frac{\mathrm{d}}{\mathrm{d}t}\int \left(\frac{\zeta^2}{\beta + \mathcal{Z}_y}\right) \mathrm{d}x \, \mathrm{d}y = 0. \tag{9.55}$$

If there is to be an instability ζ must grow, but the integral is identically zero. These two conditions can only be simultaneously satisfied if $\beta + \mathcal{Z}_y$, or equivalently $\beta - U_{yy}$, is zero somewhere in the domain.

This derivation shows that the inflection-point criterion applies even if disturbances are not of normal-mode form. The quantity $\zeta^2/(\beta + \mathcal{Z}_y)$ is an example of a *wave-activity density* — a wave activity being a conserved quantity, quadratic in the amplitude of the wave. Such quantities play an important role in instabilities, and we consider then further in Chapter 10.

9.3.2 Fjørtoft's Criterion

Another necessary condition for instability was obtained by Fjørtoft.[6] In this section we will derive his condition for normal-mode disturbances, and provide a more general derivation in Section 10.7. From the real part of (9.49) we find

$$\int_{y_1}^{y_2} (\beta - U_{yy}) \frac{(U - c_r)}{|U - c|^2} |\widetilde{\psi}|^2 \, \mathrm{d}y = \int_{y_1}^{y_2} \left| \frac{\partial \widetilde{\psi}}{\partial y} \right|^2 + k^2 |\widetilde{\psi}|^2 \, \mathrm{d}y > 0. \tag{9.56}$$

Now, from (9.50), we know that for an instability we must have

$$\int_{y_1}^{y_2} \frac{\beta - U_{yy}}{|U - c|^2} |\widetilde{\psi}|^2 \, \mathrm{d}y = 0. \tag{9.57}$$

Using this equation and (9.56) we see that, for an instability,

$$\int_{y_1}^{y_2} (\beta - U_{yy}) \frac{(U - U_s)}{|U - c|^2} |\widetilde{\psi}|^2 \, \mathrm{d}y > 0, \tag{9.58}$$

where U_s is *any* real constant. It is most useful to choose this constant to be the value of $U(y)$ at which $\beta - U_{yy}$ vanishes. This leads directly to the criterion:

> *A necessary condition for instability is that the expression*
>
> $$(\beta - U_{yy})(U - U_s)\,,$$
>
> *where U_s is the value of $U(y)$ at which $\beta - U_{yy}$ vanishes, be positive somewhere in the domain.*

This criterion is satisfied if the magnitude of the vorticity has an extremum inside the domain, and not at the boundary or at infinity (Fig. 9.8). Why choose U_s in the manner we did? Suppose we chose U_s to have a large positive value, so that $U - U_s$ is negative everywhere. Then (9.58) just implies that $\beta - U_{yy}$ must be negative somewhere, and this is already known from Rayleigh's criterion. If we choose U_s to be large and negative, we simply find that $\beta - U_{yy}$ must be positive somewhere. The most stringent criterion is obtained by choosing U_s to be the value of $U(y)$ at which $\beta - U_{yy}$ vanishes.

Interestingly, the β-effect can be either stabilizing or destabilizing: It can stabilize the middle two profiles of Fig. 9.8, because if it is large enough $\beta - U_{yy}$ will be one-signed. However, the β-effect will destabilize a westward point jet, $U(y) = -(1 - |y|)$ (the negative of the jet in Fig. 9.3), because $\beta - U_{yy}$ is negative at $y = 0$ and positive elsewhere. An eastward point jet is stable, with or without β. Finally, we emphasize that both Fjørtoft's and Rayleigh's criteria are necessary conditions for instability, and examples exist that do satisfy their criterion, yet which are stable to infinitesimal perturbations.

9.4 BAROCLINIC INSTABILITY

Baroclinic instability is a hydrodynamic instability that occurs in stably stratified, rotating fluids, and it is ubiquitous in the Earth's atmosphere and oceans, and almost certainly occurs in other planetary atmospheres. It gives rise to weather, and so is perhaps the form of hydrodynamic instability that affects us most, and that certainly we talk about most.

9.4.1 A Physical Picture

We will first draw a picture of baroclinic instability as a form of 'sloping convection' in which the fluid, although statically stable, is able to release available potential energy when parcels move along

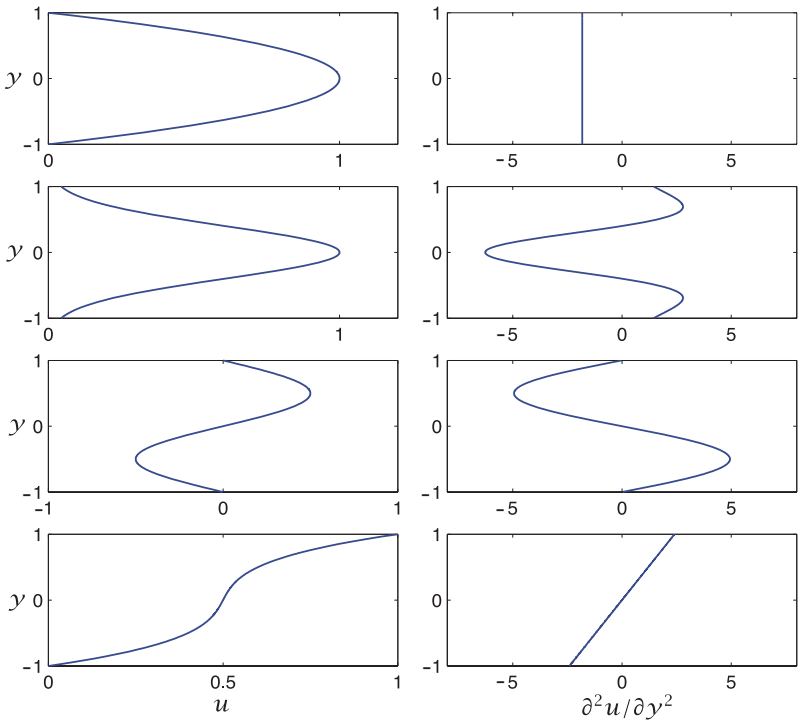

Fig. 9.8 Example parallel velocity profiles (left column) and their second derivatives (right column). From the top: Poiseuille flow ($u = 1 - y^2$); a Gaussian jet; a sinusoidal profile; a polynomial profile.

By Rayleigh's criterion, the top profile is stable, whereas the lower three are potentially unstable. However, the bottom profile is stable by Fjørtoft's criterion (note that the vorticity maxima are at the boundaries). If the β-effect were present and large enough it would stabilize the middle two profiles.

a sloping path. To this end, let us first ask: what is the basic state that is baroclinically unstable? In a stably stratified fluid potential density decreases with height; we can also easily imagine a state in which the basic state temperature decreases, and the potential density increases, polewards. (We will couch most of our discussion in terms of the Boussinesq equations, and henceforth drop the qualifier 'potential' from density.) Can we construct a steady solution from these two conditions? The answer is yes, provided the fluid is also rotating; rotation is necessary because the meridional temperature gradient generally implies a meridional pressure gradient; there is nothing to balance this in the absence of rotation, and a fluid parcel would therefore accelerate. In a rotating fluid this pressure gradient can be balanced by the Coriolis force and a steady solution can be maintained even in the absence of viscosity. Consider a stably stratified Boussinesq fluid in geostrophic and hydrostatic balance on an f-plane, with buoyancy decreasing uniformly polewards. Then $fu = -\partial\phi/\partial y$ and $\partial\phi/\partial z = b$, where $b = -g\delta\rho/\rho_0$ is the buoyancy. These together give the thermal wind relation, $\partial u/\partial z = \partial b/\partial y$. If there is no variation of these fields in the zonal direction, then, for *any* variation of b with y, this is a steady solution to the primitive equations of motion, with $v = w = 0$.

The density structure corresponding to a uniform increase of density in the meridional direction is illustrated in Fig. 9.9. Is this structure stable to perturbations? The answer is no, although the perturbations must be a little special. Suppose the particle at 'A' is displaced upwards; then, since the fluid is (by assumption) stably stratified it will be denser than its surroundings and hence experience a restoring force, and similarly if displaced downwards. Suppose, however, we interchange the two parcels at positions 'A' and 'B'. Parcel 'A' finds itself surrounded by parcels of higher density that itself, and it is therefore buoyant; it is also higher than where it started. Parcel 'B' is negatively buoyant, and at a lower altitude than where is started. Thus, overall, the centre of gravity of the fluid has been lowered, and so its overall potential energy lowered. This loss in potential energy (PE) of the basic state must be accompanied by a gain in kinetic energy of the perturbation. Thus, the perturbation amplifies and converts potential energy into kinetic energy.

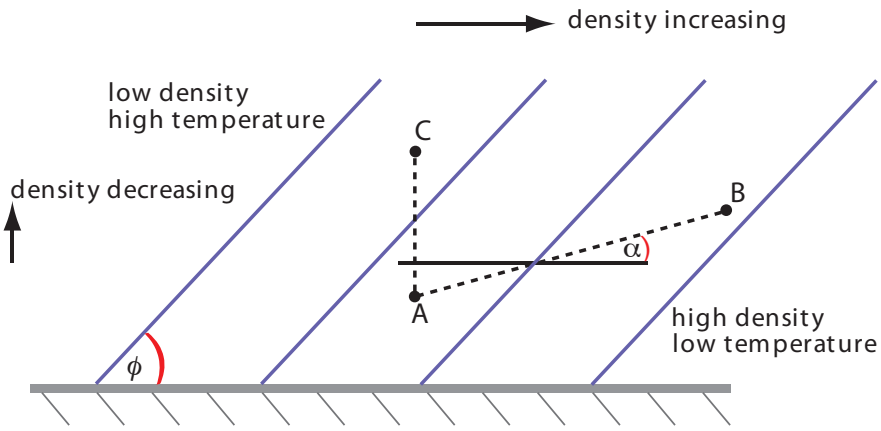

Fig. 9.9 A steady basic state giving rise to baroclinic instability. Potential density decreases upwards and equatorwards, and the associated horizontal pressure gradient is balanced by the Coriolis force. Parcel 'A' is heavier than 'C', and so statically stable, but it is lighter than 'B'. Hence, if 'A' and 'B' are interchanged there is a release of potential energy.

The loss of potential energy is easily calculated. Since

$$\mathrm{PE} = \int \rho g \, \mathrm{d}z, \tag{9.59}$$

the change in potential energy due to the interchange is

$$\Delta\mathrm{PE} = g(\rho_A z_A + \rho_B z_B - \rho_A z_B - \rho_B z_A) = g(z_A - z_B)(\rho_A - \rho_B) = g\,\Delta\rho\,\Delta z. \tag{9.60}$$

If both $\rho_B > \rho_A$ and $z_B > z_A$ then the initial potential energy is larger than the final one, energy is released and the state is unstable. If the slope of the isopycnals is ϕ [so that $\phi = -(\partial_y \rho)/(\partial_z \rho)$] and the slope of the displacements is α, then for a displacement of horizontal distance L the change in potential energy is given by

$$\Delta\mathrm{PE} = g\Delta\rho\Delta z = g\left(L\frac{\partial\rho}{\partial y} + L\alpha\frac{\partial\rho}{\partial z}\right)\alpha L = gL^2\alpha\frac{\partial\rho}{\partial y}\left(1 - \frac{\alpha}{\phi}\right), \tag{9.61}$$

if α and ϕ are small. If $0 < \alpha < \phi$ then energy is released by the perturbation, and it is maximized when $\alpha = \phi/2$. For the atmosphere the actual slope of the isotherms is about 10^{-3}, so that the slope and potential parcel trajectories are indeed shallow.

Although intuitively appealing, the thermodynamic arguments presented in this section pay no attention to satisfying the dynamical constraints of the equations of motion, and we now turn our attention to that.

9.4.2 Linearized Quasi-Geostrophic Equations

To explore the dynamics of baroclinic instability we use the quasi-geostrophic equations, specifically a potential vorticity equation for the fluid interior and a buoyancy or temperature equation at two vertical boundaries, one representing the ground and the other the tropopause. (The tropopause is the boundary between the troposphere and stratosphere at about 10 km; it is not a true rigid surface, but the higher static stability of the stratosphere inhibits vertical motion. We discuss

the effects of that in Section 9.9.) For a Boussinesq fluid, the potential vorticity equation is

$$\begin{aligned} &\frac{\partial q}{\partial t} + \boldsymbol{u}\cdot\nabla q = 0, \qquad 0 < z < H, \\ &q = \nabla^2\psi + \beta y + \frac{\partial}{\partial z}\left(F\frac{\partial \psi}{\partial z}\right), \end{aligned} \tag{9.62}$$

where $F = f_0^2/N^2$, and the buoyancy equation, with $w = 0$, is

$$\begin{aligned} &\frac{\partial b}{\partial t} + \boldsymbol{u}\cdot\nabla b = 0, \qquad z = 0, H, \\ &b = f_0\frac{\partial \psi}{\partial z}. \end{aligned} \tag{9.63}$$

A solution of these equations is a purely zonal flow, $\boldsymbol{u} = U(y,z)\mathbf{i}$ with a corresponding temperature field given by thermal wind balance. The potential vorticity of this basic state is

$$Q = \beta y - \frac{\partial U}{\partial y} + \frac{\partial}{\partial z}F\frac{\partial \Psi}{\partial z} = \beta y + \frac{\partial^2\Psi}{\partial y^2} + \frac{\partial}{\partial z}F\frac{\partial \Psi}{\partial z}, \tag{9.64}$$

where Ψ is the streamfunction of the basic state, related to U by $U = -\partial\Psi/\partial y$. Linearizing (9.62) about this zonal flow gives the potential vorticity equation for the interior,

$$\frac{\partial q'}{\partial t} + U\frac{\partial q'}{\partial x} + v'\frac{\partial Q}{\partial y} = 0, \qquad 0 < z < H, \tag{9.65}$$

where $q' = \nabla^2\psi' + \partial_z\left(F\partial_z\psi'\right)$ and $v' = \partial_x\psi'$. Similarly, the linearized buoyancy equation at the boundary is

$$\frac{\partial b'}{\partial t} + U\frac{\partial b'}{\partial x} + v'\frac{\partial B}{\partial y} = 0, \qquad z = 0, H, \tag{9.66}$$

where $b' = f_0\partial_z\psi'$ and $\partial_y B = \partial_y(f_0\partial_z\Psi) = -f_0\partial U/\partial z$.

Just as for the barotropic problem, a standard way of proceeding is to seek normal-mode solutions. Since the coefficients of (9.65) and (9.66) are functions of y and z, but not of x, we seek solutions of the form

$$\psi'(x,y,z,t) = \mathrm{Re}\,\tilde{\psi}(y,z)\mathrm{e}^{\mathrm{i}k(x-ct)}, \tag{9.67}$$

and similarly for the derived quantities u', v', b' and q'. In particular,

$$\tilde{q} = \frac{\partial^2\tilde{\psi}}{\partial y^2} + \frac{\partial}{\partial z}F\frac{\partial\tilde{\psi}}{\partial z} - k^2\tilde{\psi}. \tag{9.68}$$

Using (9.68) and (9.67) in (9.65) and (9.66) gives, with subscripts y and z denoting derivatives,

$$(U-c)\left(\tilde{\psi}_{yy} + (F\tilde{\psi}_z)_z - k^2\tilde{\psi}\right) + Q_y\tilde{\psi} = 0 \qquad 0 < z < H, \tag{9.69a}$$

$$(U-c)\tilde{\psi}_z - U_z\tilde{\psi} = 0 \qquad z = 0,\ H. \tag{9.69b}$$

These equations are analogous to Rayleigh's equations for parallel shear flow, and illustrate the similarity between the baroclinic instability problem and that of a parallel shear flow.

9.4.3 Necessary Conditions for Baroclinic Instability

Necessary conditions for instability may be obtained (as for parallel shear flows) by multiplying (9.69) by $\tilde{\psi}^*$ and integrating over the domain. Integrating by parts, we first note that

$$\int_{y_1}^{y_2} \tilde{\psi}^* \tilde{\psi}_{yy}\,\mathrm{d}y = \left[\tilde{\psi}^* \tilde{\psi}_y\right]_{y_1}^{y_2} - \int_{y_1}^{y_2} |\tilde{\psi}_y|^2\,\mathrm{d}y. \tag{9.70}$$

If the integral is performed between two quiescent latitudes, or $\psi = 0$ at the meridional boundaries, then the first term on the right-hand side vanishes. Similarly,

$$\begin{aligned}\int_0^H \tilde{\psi}^* (F\tilde{\psi}_z)_z\,\mathrm{d}z &= \left[F\tilde{\psi}^* \tilde{\psi}_z\right]_0^H - \int_0^H F|\tilde{\psi}_z|^2\,\mathrm{d}z \\ &= \left[\frac{FU_z|\tilde{\psi}|^2}{(U-c)}\right]_0^H - \int_0^H F|\tilde{\psi}_z|^2\,\mathrm{d}z,\end{aligned} \tag{9.71}$$

using (9.69b). Now, multiply (9.69a) by $\tilde{\psi}^*$ and integrate over y and z, and use (9.70) and (9.71) to obtain

$$\int_0^H \int_{y_1}^{y_2} |\psi_y|^2 + F|\tilde{\psi}_z|^2 + k^2|\tilde{\psi}|^2]\,\mathrm{d}y\,\mathrm{d}z - \int_{y_1}^{y_2} \left\{\int_0^H \frac{Q_y}{U-c}|\tilde{\psi}|^2\,\mathrm{d}z + \left[\frac{FU_z|\tilde{\psi}|^2}{U-c}\right]_0^H\right\}\,\mathrm{d}y = 0. \tag{9.72}$$

The first term is purely real whereas the second term is complex. The imaginary component of the second term must be zero and therefore

$$-c_\mathrm{i} \int_{y_1}^{y_2} \left\{\int_0^H \frac{Q_y}{|U-c|^2}|\tilde{\psi}|^2\,\mathrm{d}z + \left[\frac{FU_z|\tilde{\psi}|^2}{|U-c|^2}\right]_0^H\right\}\,\mathrm{d}y = 0. \tag{9.73}$$

If there is to be instability c_i must be non-zero and the integrand must therefore vanish. This gives the *Charney–Stern–Pedlosky* (CSP) necessary condition for instability,[7] namely that one of the following criteria must be satisfied:

(i) Q_y changes sign in the interior.
(ii) Q_y is the opposite sign to U_z at the upper boundary, $z = H$.
(iii) Q_y is the same sign as U_z at the lower boundary, $z = 0$.
(iv) U_z is the same sign at the upper and lower boundaries, a condition that differs from *(ii)* or *(iii)* if $Q_y = 0$.

In the Earth's mid-latitude atmosphere, Q_y is often dominated by β, and is positive everywhere, as, frequently, is the shear. The instability criterion is then normally satisfied through *(iii)*: that is, both Q_y and $U_z(0)$ are positive. A more general, and in some ways simpler, derivation that does not rely on normal-mode disturbances is given in Section 10.7.2.

9.5 THE EADY PROBLEM

We now proceed to explicitly calculate the stability properties of a particular configuration that has become known as the *Eady problem.* This was one of the first two mathematical descriptions of baroclinic instability, the other being the *Charney problem.*[8] The two problems were formulated independently, each being the (largely unsupervised) PhD thesis of its author, and although the Charney problem is in some respects more complete (for example in allowing a β-effect), the Eady problem displays the instability in a more transparent form. The Charney problem in its entirety is also quite mathematically opaque, and so we first consider the Eady problem.[9] The β-effect can be incorporated relatively simply in the two-layer model of the next section, and in Section 9.9.1 we look at some aspects of the Charney problem approximately. To begin, let us make the following simplifying assumptions:

(i) The motion is on the f-plane ($\beta = 0$). This assumption, although not particularly realistic for the Earth's atmosphere, greatly simplifies the analysis.

(ii) The fluid is uniformly stratified; that is, N^2 is a constant. This is a decent approximation for the atmosphere below the tropopause, but less so for the ocean where the stratification varies considerably, being much larger in the upper ocean.

(iii) The basic state has uniform shear; that is, $U_0(z) = \Lambda z = Uz/H$, where Λ is the (constant) shear and U is the zonal velocity at $z = H$, where H is the domain depth. This profile is more appropriate for the atmosphere than the ocean — below the thermocline the ocean is relatively quiescent and the shear is small.

(iv) The motion is contained between two rigid, flat horizontal surfaces. In the atmosphere this corresponds to the ground and a 'lid' at a constant-height tropopause.

Although, apart from *(i)*, these assumptions are more appropriate for the atmosphere than the ocean, the same qualitative nature of baroclinic instability carries through to the ocean.

9.5.1 The Linearized Problem

With a basic state streamfunction of $\Psi = -\Lambda z y$, the basic state potential vorticity, Q, is

$$Q = \nabla^2\Psi + \frac{H^2}{L_d^2}\frac{\partial}{\partial z}\left(\frac{\partial \Psi}{\partial z}\right) = 0. \tag{9.74}$$

The fact that $Q = 0$ makes the Eady problem a special case, albeit an illuminating one. The linearized potential vorticity equation is

$$\left(\frac{\partial}{\partial t} + \Lambda z\frac{\partial}{\partial x}\right)\left(\nabla^2\psi' + \frac{H^2}{L_d^2}\frac{\partial^2\psi'}{\partial z^2}\right) = 0. \tag{9.75}$$

This equation has no x-dependent coefficients and in a periodic channel we may seek solutions of the form $\psi'(x, y, z, t) = \mathrm{Re}\,\tilde{\psi}(y, z)\mathrm{e}^{\mathrm{i}k(x-ct)}$, yielding

$$(\Lambda z - c)\left(\frac{\partial^2\tilde{\psi}}{\partial y^2} + \frac{H^2}{L_d^2}\frac{\partial^2\tilde{\psi}}{\partial z^2} - k^2\tilde{\psi}\right) = 0. \tag{9.76}$$

This equation is (9.69a) applied to the Eady problem.

Boundary conditions

There are two sets of boundary conditions to satisfy, the vertical boundary conditions at $z = 0$ and $z = H$ and the lateral boundary conditions. In the horizontal plane we may either consider the flow to in a channel, periodic in x and confined between two meridional walls, or, with a slightly greater degree of idealization but with little change to the essential dynamics, we may suppose that the domain is doubly-periodic. Either case is dealt with easily enough by the choice of geometric basis function; we choose a channel of width L and impose $\psi = 0$ at $y = +L/2$ and $y = -L/2$ and, to satisfy this, seek solutions of the form $\Psi = \Phi(z)\sin ly$ or, using (9.67)

$$\psi'(x, y, z, t) = \mathrm{Re}\,\Phi(z)\sin ly\,\mathrm{e}^{\mathrm{i}k(x-ct)}, \tag{9.77}$$

where $l = n\pi/L$, with n being a positive integer.

The vertical boundary conditions are that $w = 0$ at $z = 0$ and $z = H$. We follow the procedure of Section 9.4.2 and from (9.66) we obtain

$$\left(\frac{\partial}{\partial t} + \Lambda z\frac{\partial}{\partial x}\right)\frac{\partial\psi'}{\partial z} - \Lambda\frac{\partial\psi'}{\partial x} = 0, \qquad \text{at } z = 0, H. \tag{9.78}$$

Solutions

Substituting (9.77) into (9.76) gives the interior potential vorticity equation

$$(\Lambda z - c)\left[\frac{H^2}{L_d^2}\frac{\partial^2\Phi}{\partial z^2} - (k^2 + l^2)\Phi\right] = 0, \tag{9.79}$$

and substituting (9.77) into (9.78) gives, at $z = 0$ and $z = H$,

$$c\frac{\mathrm{d}\Phi}{\mathrm{d}z} + \Lambda\Phi = 0 \qquad \text{and} \qquad (c - \Lambda H)\frac{\mathrm{d}\Phi}{\mathrm{d}z} + \Lambda\Phi = 0. \tag{9.80a,b}$$

These are equivalent to (9.69b) applied to the Eady problem. If $\Lambda z \neq c$ then (9.79) becomes[10]

$$H^2\frac{\mathrm{d}^2\Phi}{\mathrm{d}z^2} - \mu^2\Phi = 0, \tag{9.81}$$

where $\mu^2 = L_d^2(k^2 + l^2)$. The nondimensional parameter μ is a horizontal wavenumber, scaled by the inverse of the Rossby radius of deformation. Solutions of (9.81) are

$$\Phi(z) = A\cosh\mu\hat{z} + B\sinh\mu\hat{z}, \tag{9.82}$$

where $\hat{z} = z/H$; thus, μ determines the vertical structure of the solution. The boundary conditions (9.80) are satisfied if

$$\begin{gathered} A\,[\Lambda H] + B\,[\mu c] = 0, \\ A\,[(c - \Lambda H)\mu\sinh\mu + \Lambda H\cosh\mu] + B\,[(c - \Lambda H)\mu\cosh\mu + \Lambda H\sinh\mu] = 0. \end{gathered} \tag{9.83}$$

Equations (9.83) are two coupled homogeneous equations in the two unknowns A and B. Non-trivial solutions will only exist if the determinant of their coefficients (the terms in square brackets) vanishes, and this leads to

$$c^2 - Uc + U^2(\mu^{-1}\coth\mu - \mu^{-2}) = 0, \tag{9.84}$$

where $U \equiv \Lambda H$ and $\coth\mu = \cosh\mu/\sinh\mu$. The solution of (9.84) is

$$c = \frac{U}{2} \pm \frac{U}{\mu}\left[\left(\frac{\mu}{2} - \coth\frac{\mu}{2}\right)\left(\frac{\mu}{2} - \tanh\frac{\mu}{2}\right)\right]^{1/2}. \tag{9.85}$$

The waves, being proportional to $\exp(-\mathrm{i}kct)$, will grow exponentially if c has an imaginary part. Since $\mu/2 > \tanh(\mu/2)$ for all μ, for an instability we require that

$$\frac{\mu}{2} < \coth\frac{\mu}{2}, \tag{9.86}$$

which is satisfied when $\mu < \mu_c$ where $\mu_c = 2.399$. The growth rates of the instabilities themselves are given by the imaginary part of (9.85), multiplied by the x-wavenumber; that is

$$\sigma = kc_i = k\frac{U}{\mu}\left[\left(\coth\frac{\mu}{2} - \frac{\mu}{2}\right)\left(\frac{\mu}{2} - \tanh\frac{\mu}{2}\right)\right]^{1/2}. \tag{9.87}$$

These solutions suggest a natural nondimensionalization: scale length by L_d, height by H and time by $L_d/U = L_d/(H\Lambda)$. The growth rate scales as the inverse of the time scaling and so by U/L_d. The timescale is also usefully written as

$$T_E = \frac{L_d}{U} = \frac{NH}{f_0 U} = \frac{N}{f_0\Lambda} = \frac{1}{Rif_0} = \frac{\sqrt{Ri}}{f_0}, \tag{9.88}$$

where $Fr = U/(NH)$ and $Ri = N^2/\Lambda^2$ are the Froude and Richardson numbers for this problem.

From (9.87) we can (with a little work) determine that the maximum growth rate occurs when $\mu = \mu_m = 1.61$. For any given x-wavenumber, the most unstable wavenumber has the gravest meridional scale, which here is $n = 1$, and we may further consider a wide channel so that $l^2 \ll k^2$. The maximum growth rate, σ_E, is then given by

$$\sigma_E = \frac{0.31U}{L_d} = \frac{0.31\Lambda H}{L_d} = \frac{0.31\Lambda f}{N}, \tag{9.89}$$

and this is known as the *Eady growth rate*. We have removed the subscript 0 from the Coriolis parameter here. Although f is taken as constant in the quasi-geostrophic derivation, we might wish to calculate the Eady growth rate at various locations around the globe, in which case we should use the local value of the Coriolis parameter and deformation radius. Evidently, the growth rate is proportional to the shear times the Prandtl ratio, f/N. The associate phase speed is the real part of c and is given by $c_r = 0.5U$.

For small l the unstable x-wavenumbers and corresponding wavelengths occur for

$$k < k_c = \frac{\mu_c}{L_d} = \frac{2.4}{L_d}, \qquad \lambda > \lambda_c = \frac{2\pi L_d}{\mu_c} = 2.6L_d. \tag{9.90a,b}$$

The wavenumber and wavelength at which the instability is greatest are:

$$k_m = \frac{1.6}{L_d}, \qquad \lambda_m = \frac{2\pi L_d}{\mu_m} = 3.9L_d. \tag{9.91a,b}$$

These properties are illustrated in the left-hand panels of Fig. 9.10 and in Fig. 9.11.

Given c, we may use (9.83) to determine the vertical structure of the Eady wave and this is, to within an arbitrary constant factor,

$$\Phi(\hat{z}) = \cosh\mu\hat{z} - \frac{U}{\mu c}\sinh\mu\hat{z} = \left(\cosh\mu\hat{z} - \frac{Uc_r\sinh\mu\hat{z}}{\mu|c^2|} + \frac{\mathrm{i}Uc_i\sinh\mu\hat{z}}{\mu|c^2|}\right). \tag{9.92}$$

The wave therefore has a phase, $\theta(z)$, given by

$$\theta(\hat{z}) = \tan^{-1}\left(\frac{Uc_i\sinh\mu\hat{z}}{\mu|c^2|\cosh\mu\hat{z} - Uc_r\sinh\mu\hat{z}}\right). \tag{9.93}$$

The phase and amplitude of the Eady waves are plotted in the right panels of Fig. 9.10, and their overall structure in Fig. 9.12, where we see the unstable wave tilting into the shear.

9.5.2 Atmospheric and Oceanic Parameters

To get a qualitative sense of the nature of the instability we choose some typical parameters, as follows.

For the atmosphere

Let us choose

$$H \sim 10\,\mathrm{km}, \qquad U \sim 10\,\mathrm{m\,s^{-1}}, \qquad N \sim 10^{-2}\,\mathrm{s^{-1}}. \tag{9.94}$$

We then obtain:

$$\text{deformation radius:} \qquad L_d = \frac{NH}{f} \approx \frac{10^{-2}\,10^4}{10^{-4}} \approx 1000\,\mathrm{km}, \tag{9.95}$$

$$\text{scale of maximum instability:} \qquad L_{\max} \approx 3.9L_d \approx 4000\,\mathrm{km}, \tag{9.96}$$

$$\text{growth rate:} \qquad \sigma \approx 0.3\frac{U}{L_d} \approx \frac{0.3\times 10}{10^6}\,\mathrm{s^{-1}} \approx 0.26\,\mathrm{day^{-1}}. \tag{9.97}$$

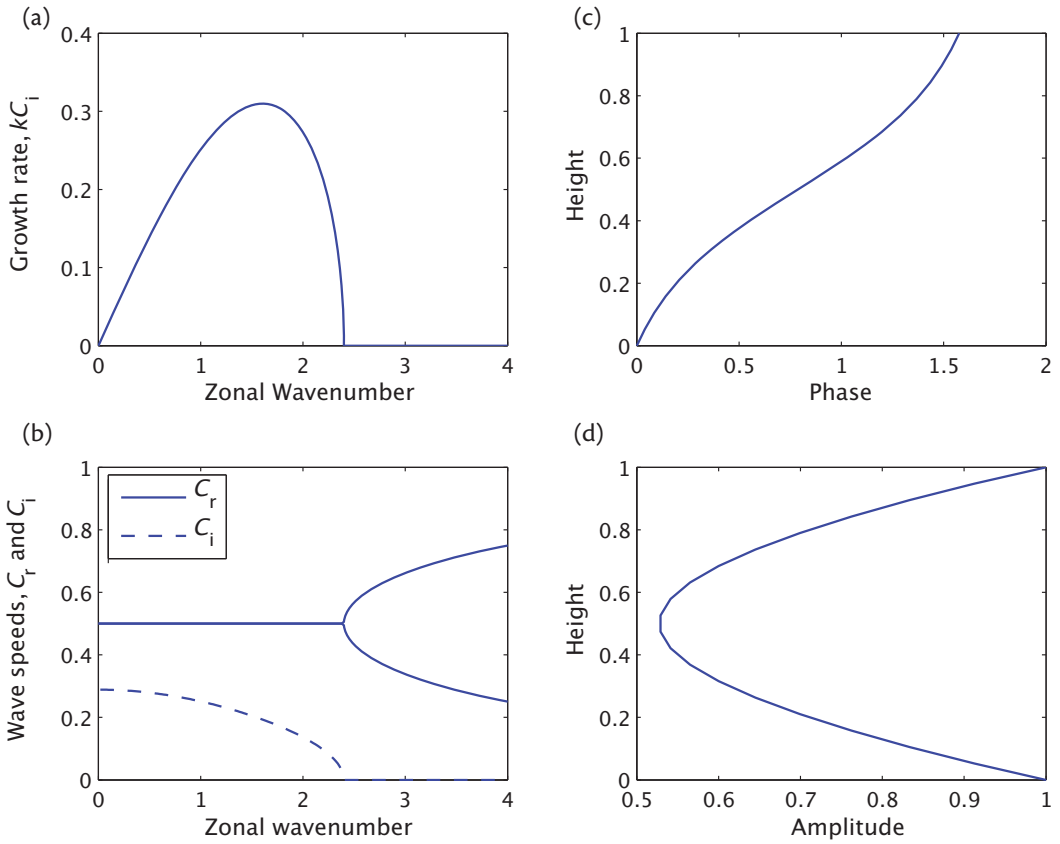

Fig. 9.10 Solution of the Eady problem, in nondimensional units. (a) The growth rate, kc_i as a function of scaled wavenumber μ, from (9.87) with $\Lambda = H = 1$ and for the gravest meridional mode. (b) The real (solid) and imaginary (dashed) wave speeds of those modes, as a function of horizontal wavenumber. (c) The phase of the single most unstable mode as a function of height. (d) The amplitude of that mode as a function of height. To obtain dimensional values, multiply the growth rate by $\Lambda H/L_d$ and the wavenumber by $1/L_d$.

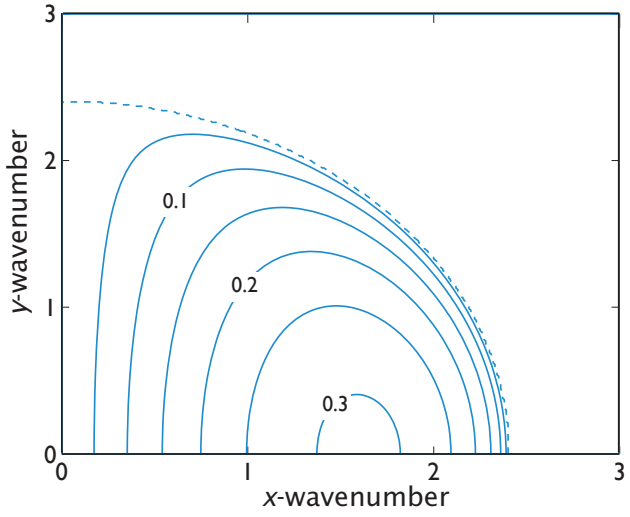

Fig. 9.11 Contours of the growth rate, σ, in the Eady problem, in the k–l plane using (9.87), nondimensionalized as in Fig. 9.10. The growth rate peaks near the deformation scale, and for any given zonal wavenumber the most unstable wavenumber is that with the gravest meridional scale.

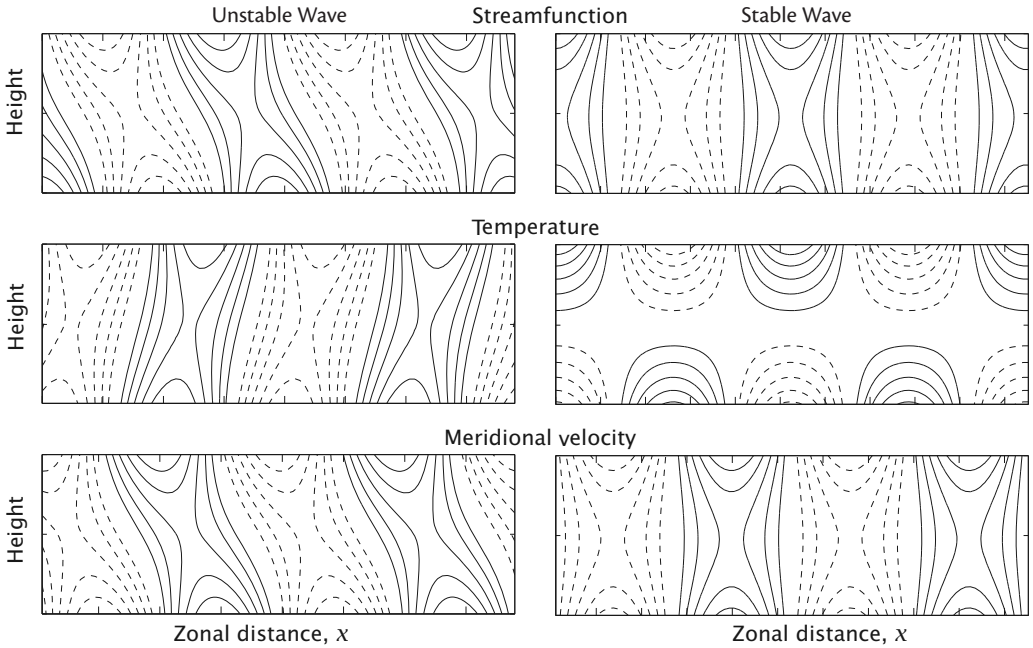

Fig. 9.12 Left column: vertical structure of the most unstable Eady mode. Top: contours of streamfunction. Middle: temperature, $\partial\psi/\partial z$. Bottom: meridional velocity, $\partial\psi/\partial x$. Negative contours are dashed, and two complete wavelengths are present in the horizontal direction. Polewards flowing (positive v) air is generally warmer than equatorwards flowing air. Right column: the same, but now for a wave just beyond the short-wave cut-off.

For the ocean

For the main thermocline in the ocean let us choose

$$H \sim 1\,\text{km}, \qquad U \approx 0.1\,\text{m}\,\text{s}^{-1}, \qquad N \sim 10^{-2}\,\text{s}^{-1}. \tag{9.98}$$

We then obtain:

$$\text{deformation radius:} \qquad L_d = \frac{NH}{f} \approx \frac{10^{-2}\times 1000}{10^{-4}} = 100\,\text{km}, \tag{9.99}$$

$$\text{scale of maximum instability:} \qquad L_{\max} \approx 3.9\,L_d \approx 400\,\text{km}, \tag{9.100}$$

$$\text{growth rate:} \qquad \sigma \approx 0.3\frac{U}{L_d} \approx \frac{0.3\times 0.1}{10^5}\,\text{s}^{-1} \approx 0.026\,\text{day}^{-1}. \tag{9.101}$$

In the ocean, the Eady problem is not quantitatively applicable because of the non-uniformity of the stratification. Nevertheless, the above estimates give a qualitative sense of the scale and growth rate of the instability relative to the corresponding values in the atmosphere. A summary of the main points of the Eady problem is given in the shaded box on the facing page.

9.6 TWO-LAYER BAROCLINIC INSTABILITY

The eigenfunctions displaying the largest growth rates in the Eady problem have a relatively simple vertical structure. This suggests that an even simpler mathematical model of baroclinic instability might be constructed in which the vertical structure is a priori restricted to a very simple form, namely the two-layer or two-level quasi-geostrophic (QG) model of Sections 5.3.2 and 5.4.6. This

Some Results in Baroclinic Instability

Eady Problem

- The length scales of the instability are characterized by the deformation scale. The most unstable scale has a wavelength about four times the deformation radius L_d, where $L_d = NH/f$.
- The growth rate of the instability is approximately

$$\sigma_E \approx \frac{0.3U}{L_d} = 0.3\Lambda\frac{f}{N}. \tag{B.1}$$

  That is, it is proportional to the shear scaled by the Prandtl ratio f/N. The value σ_E is known as the *Eady growth rate.*
- The most unstable waves for a given zonal scale are those with the gravest meridional scale.
- There is a *short-wave cutoff* beyond which (i.e., at higher wavenumber than) there is no instability. This occurs near the deformation radius.
- The instability relies on an interaction between waves at the upper and lower boundaries. If either boundary is removed, the instability dies. This point is considered in Section 9.7.
- The two-layer (Phillips) problem with zero beta captures many of the results of the Eady model.

Effects of beta

- The beta effect allows the instability to grow by the interaction of edge waves at the surface with Rossby waves in the interior, not just with edge waves at the top. Potential vorticity changes sign because of an interaction between the surface temperature gradient and the interior potential vorticity gradient. Thus, not all unstable modes are deep.
- There is a long-wave cut-off to the main instability branch. At scales larger than this the instabilities are slowly growing, and absent in the two-layer (Phillips) problem.
- In the continuously stratified problem there is no short wave cut-off, but these modes are slowly growing and in the two-layer model they are absent.
- In the two-layer model with beta, there is a minimum shear, Λ_c, for instability given by

$$\Lambda_c = \frac{\beta H}{2}\frac{N^2}{f^2}. \tag{B.2}$$

  This shear does not arise in the continuous problem, although it may be a useful criterion for the onset of rapidly growing deep modes.
- The above differences between the two-layer problem and the continuously stratified one arise because in the former all modes are deep and so there can be no interaction between edge waves and shallow Rossby waves.

instability problem is often called the 'Phillips problem'.[11] One notable advantage over the Eady model is that it is possible to include the β-effect in a simple way.

9.6.1 Posing the Problem

For two layers or two levels of equal thickness, we write the potential vorticity equations in the dimensional form,

$$\frac{\mathrm{D}}{\mathrm{D}t}\left[\zeta_i + \beta y + \frac{k_d^2}{2}(\psi_j - \psi_i)\right] = 0, \qquad i = 1,2, \quad j = 3-i, \tag{9.102}$$

where, using two-level notation for definiteness,

$$\frac{k_d^2}{2} = \left(\frac{2f_0}{NH}\right)^2 \quad \rightarrow \quad k_d = \frac{\sqrt{8}}{L_d}, \tag{9.103}$$

where H is the total depth of the domain, as in the Eady problem. The basic state we choose is

$$\Psi_1 = -U_1 y, \qquad \Psi_2 = -U_2 y = +U_1 y. \tag{9.104}$$

It is possible to choose $U_2 = -U_1$ without loss of generality because there is no topography and the system is Galilean invariant. The basic state potential vorticity gradient is then given by

$$Q_1 = \beta y + k_d^2 U y, \qquad Q_2 = \beta y - k_d^2 U y, \tag{9.105}$$

where $U = U_1$. (Note that U differs by a constant multiplicative factor from the U in the Eady problem.) Even in the absence of β there is a non-zero potential vorticity gradient. Why should this be different from the Eady problem? — after all, the shear is uniform in both problems. The difference arises from the vertical boundary conditions. In the standard layered formulation the temperature gradient at the boundary is absorbed into the definition of the potential vorticity in the interior. This results in a non-zero interior potential vorticity gradient at the two levels adjacent to the boundary (the only layers in the two-layer problem), but with isothermal boundary conditions $\mathrm{D}(\partial\psi/\partial z)/\mathrm{D}t = 0$. In the Eady problem we have a zero interior gradient of potential vorticity but a temperature gradient at the boundary. The two formulations are physically equivalent — a finite-difference example of the Bretherton boundary layer, encountered in Section 5.4.3.

The linearized potential vorticity equation is, for each layer,

$$\frac{\partial q_i'}{\partial t} + U_i\frac{\partial q_i'}{\partial x} + v_i'\frac{\partial Q_i}{\partial y} = 0, \qquad i = 1,2, \tag{9.106}$$

or, more explicitly,

$$\left(\frac{\partial}{\partial t} + U\frac{\partial}{\partial x}\right)\left[\nabla^2\psi_1' + \frac{k_d^2}{2}(\psi_2' - \psi_1')\right] + \frac{\partial\psi_1'}{\partial x}(\beta + k_d^2 U) = 0, \tag{9.107a}$$

$$\left(\frac{\partial}{\partial t} - U\frac{\partial}{\partial x}\right)\left[\nabla^2\psi_2' + \frac{k_d^2}{2}(\psi_1' - \psi_2')\right] + \frac{\partial\psi_2'}{\partial x}(\beta - k_d^2 U) = 0. \tag{9.107b}$$

For simplicity we will set the problem in a square, doubly periodic domain, and so seek solutions of the form,

$$\psi_i' = \mathrm{Re}\,\widetilde{\psi}_i \mathrm{e}^{\mathrm{i}(kx+ly-\omega t)} = \mathrm{Re}\,\widetilde{\psi}_i \mathrm{e}^{\mathrm{i}k(x-ct)}\mathrm{e}^{\mathrm{i}ly}, \qquad i = 1,2. \tag{9.108}$$

Here, k and l are the x- and y-wavenumbers, and $(k,l) = (2\pi/L)(m,n)$, where L is the size of the domain, and m and n are integers. The constant $\widetilde{\psi}_i$ is the complex amplitude.

9.6.2 The Solution

Substituting (9.108) into (9.107) we obtain

$$[\mathrm{i}k(U-c)]\left[-K^2\tilde{\psi}_1 + k_d^2(\tilde{\psi}_2-\tilde{\psi}_1)/2\right] + \mathrm{i}k\tilde{\psi}_1(\beta + k_d^2 U) = 0, \tag{9.109a}$$

$$[-\mathrm{i}k(U+c)]\left[-K^2\tilde{\psi}_2 + k_d^2(\tilde{\psi}_1-\tilde{\psi}_2)/2\right] + \mathrm{i}k\tilde{\psi}_2(\beta - k_d^2 U) = 0, \tag{9.109b}$$

where $K^2 = k^2 + l^2$. Re-arranging these two equations gives

$$\left[(U-c)(k_d^2/2 + K^2) - (\beta + k_d^2 U)\right]\tilde{\psi}_1 - \left[k_d^2(U-c)/2\right]\tilde{\psi}_2 = 0, \tag{9.110a}$$

$$-\left[k_d^2(U+c)/2\right]\tilde{\psi}_1 + \left[(U+c)(k_d^2/2 + K^2) + (\beta - k_d^2 U)\right]\tilde{\psi}_2 = 0. \tag{9.110b}$$

These equations are of the form

$$[A]\tilde{\psi}_1 + [B]\tilde{\psi}_2 = 0, \qquad [C]\tilde{\psi}_1 + [D]\tilde{\psi}_2 = 0, \tag{9.111}$$

where A, B, C, D correspond to the terms in square brackets in (9.110). For non-trivial solutions the determinant of coefficients must be zero, that is $AD - BC = 0$. This gives a quadratic equation in c and solving this we obtain

$$c = -\frac{\beta}{K^2 + k_d^2}\left\{1 + \frac{k_d^2}{2K^2} \pm \frac{k_d^2}{2K^2}\left[1 + \frac{4K^4(K^4 - k_d^4)}{k_\beta^4 k_d^4}\right]^{1/2}\right\}, \tag{9.112}$$

where $K^4 = (k^2 + l^2)^2$ and $k_\beta = \sqrt{\beta/U}$ (its inverse is known as the Kuo scale). We may non-dimensionalize this equation using the deformation radius L_d as the length scale and the shear velocity U as the velocity scale.[12] Then, denoting nondimensional parameters with hats, we have

$$k = \frac{\hat{k}}{L_d}, \qquad c = \hat{c}\,U, \qquad t = \frac{L_d}{U}\hat{t}, \tag{9.113}$$

and the nondimensional form of (9.112) is just

$$\hat{c} = -\frac{\hat{k}_\beta^2}{\hat{K}^2 + \hat{k}_d^2}\left\{1 + \frac{\hat{k}_d^2}{2\hat{K}^2} \pm \frac{\hat{k}_d^2}{2\hat{K}^2}\left[1 + \frac{4\hat{K}^4(\hat{K}^4 - \hat{k}_d^4)}{\hat{k}_\beta^4 \hat{k}_d^4}\right]^{1/2}\right\}, \tag{9.114}$$

where $\hat{k}_\beta = k_\beta L_d$ and $\hat{k}_d = \sqrt{8}$, as in (9.103). The nondimensional parameter

$$\gamma = \frac{1}{4}\hat{k}_\beta^2 = \frac{\beta L_d^2}{4U}, \tag{9.115}$$

is often useful as a measure of the importance of β; it is proportional to the square of the ratio of the deformation radius to the Kuo scale $\sqrt{U/\beta}$. (It is the two-layer version of the 'Charney–Green number' considered more in Section 9.9.1.) Let us look at two special cases first, before considering the general solution to these equations.

I. Zero shear, non-zero β

If there is no shear (i.e., $U = 0$) then (9.110a) and (9.110b) are identical and two roots of the equation give the purely real phase speeds c,

$$c = -\frac{\beta}{K^2} \qquad \text{and} \qquad c = -\frac{\beta}{K^2 + k_d^2}. \tag{9.116}$$

The first of these is the dispersion relationship for Rossby waves in a purely barotropic flow, and corresponds to the eigenfunction $\tilde{\psi}_1 = \tilde{\psi}_2$. The second solution corresponds to the baroclinic eigenfunction $\tilde{\psi}_1 + \tilde{\psi}_2 = 0$.

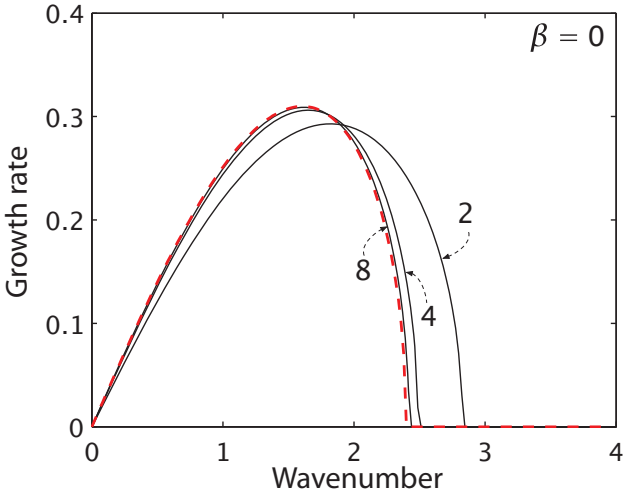

Fig. 9.13 Baroclinic growth rate as calculated with two, four and eight vertical levels (solid lines, as labelled), and in the continuous case (red dashed line), all with $\beta = 0$. The two-level result is the analytic result of (9.117), and the continuous result is the analytic result of the Eady problem. The four- and eight-level results were obtained numerically, and are almost the same as the result from the Eady problem.

II. Zero β, non-zero shear

If $\beta = 0$, then (9.110) yields, after a little algebra,

$$c = \pm U\left(\frac{K^2 - k_d^2}{K^2 + k_d^2}\right)^{1/2} \qquad \text{or} \qquad \sigma = Uk\left(\frac{k_d^2 - K^2}{K^2 + k_d^2}\right)^{1/2}, \tag{9.117}$$

where $\sigma = -\mathrm{i}\omega$ is the growth rate. These expressions are similar to those in the Eady problem. Indeed, as we increase the number of levels (using a numerical method to perform the calculation) the growth rate converges to that of the Eady problem (Fig. 9.13). We note the following:

- There is an instability for *all* values of U.
- There is a high-wavenumber cut-off, at a scale proportional to the radius of deformation. For the two-layer model, if $K > k_d = 2.82/L_d$ there is no growth. For the Eady problem, the high wavenumber cut-off occurs at $2.4/L_d$.
- There is no low wavenumber cut-off.
- For any given k, the highest growth rate occurs for $l = 0$. In the two-layer model, from (9.117), for $l = 0$ the maximum growth rate occurs when $k = 0.634k_d = 1.79/L_d$. For the Eady problem, the maximum growth rate occurs at $1.61/L_d$.

Solution in the general case: non-zero shear and non-zero β

Using (9.114), the growth rate and wave speeds as function of wavenumber are plotted in Fig. 9.14. We observe that there still appears to be a high-wavenumber cut-off and, for $\beta = 0$, there is a low-wavenumber cut-off. A little analysis elucidates the origin of these features.

The neutral curve

For instability, there must be an imaginary component to the phase speed in (9.112); that is, we require

$$k_\beta^4 k_d^4 + 4K^4(K^4 - k_d^4) < 0. \tag{9.118}$$

This is a quadratic equation in K^4 for the value of K, K_c say, at which the growth rate is zero. Solving, we find

$$K_c^4 = \frac{1}{2}k_d^4\left(1 \pm \sqrt{1 - k_\beta^4/k_d^4}\right), \tag{9.119}$$

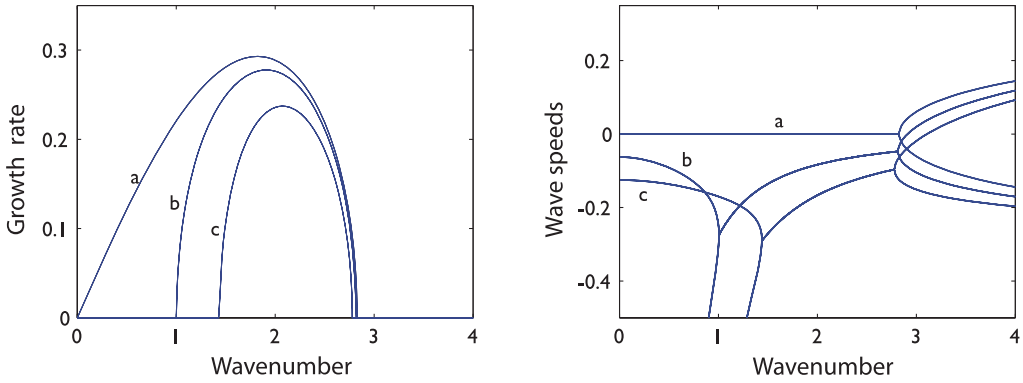

Fig. 9.14 Growth rates and wave speeds for the two-layer baroclinic instability problem, from (9.114), with three (nondimensional) values of β as labelled: a, $\gamma = 0$ ($\widehat{k}_\beta = 0$); b, $\gamma = 0.5$ ($\widehat{k}_\beta = \sqrt{2}$); c, $\gamma = 1$ ($\widehat{k}_\beta = 2$). As β increases, so does the low-wavenumber cut-off to instability, but the high-wavenumber cut-off is little changed. The solutions are obtained from (9.114), with $\widehat{k}_d = \sqrt{8}$ and $U_1 = -U_2 = 1/4$.

and this is plotted in Fig. 9.15. From (9.118) useful approximate expressions can be obtained for the critical shear as a function of wavenumber in the limits of small K and $K \approx k_d$, and these are left as exercises for the reader.

Minimum shear for instability

From (9.118), instability arises when $\beta^2 {k_d}^4/U^2 < 4K^4({k_d}^4 - K^4)$. The maximum value of the right-hand side of this expression arises when $K^4 = \widehat{k}_d^4/2$; thus, instability arises only when

$$\frac{\beta^2 k_d^4}{U^2} < 4\frac{k_d^4}{2}\frac{k_d^4}{2} \qquad \text{or} \qquad \kappa_\beta < k_d. \tag{9.120}$$

That is, *instability only arises if the deformation radius is sufficiently smaller than the Kuo scale.* The critical velocity difference required for instability is then

$$U_1 - U_2 > U_c = \frac{2\beta}{k_d^2} = \frac{1}{4}\beta L_d^2, \tag{9.121}$$

recalling our notation that $U_1 - U_2 = 2U$ and that $k_d^2 = 8/L_d^2$, as in (9.103). The critical shear for instability is

$$\Lambda_c = \frac{\beta H}{2}\frac{N^2}{f^2}, \tag{9.122a,b}$$

where the shear Λ is defined by $(U_1 - U_2)/(0.5H)$, where H is the total depth of the domain.

In any given quasi-geostrophic calculation f is held constant, but if we wish to see how the critical shear varies with latitude we vary f accordingly. Figure 9.16 sketches how this critical shear might vary with latitude in the atmosphere and ocean, allowing f to vary. If the shear is just the critical value, the instability occurs at $k = 2^{-1/4}k_d = 0.84k_d = 2.37/L_d$. As the shear increases, the wavenumber at which the growth rate is maximum decreases slightly (see Fig. 9.15), and for a sufficiently large shear the β-effect is negligible and the wavenumber of maximum instability is, as we saw earlier, $0.634\,k_d$ or $1.79/L_d$

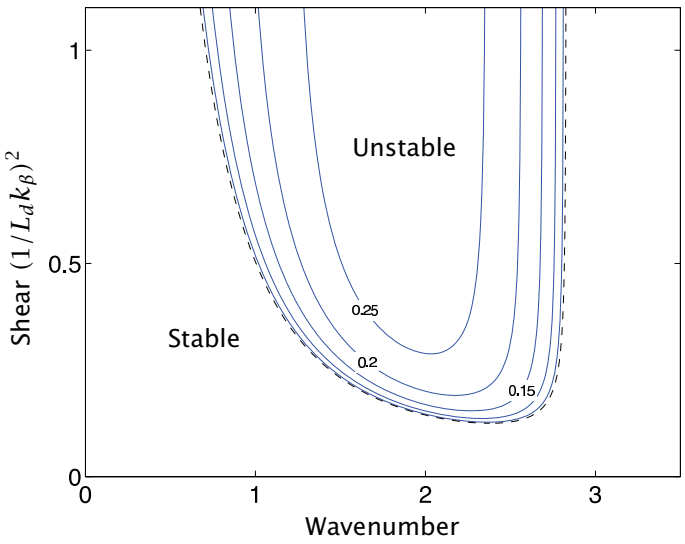

Fig. 9.15 Contours of growth rate in the two-layer baroclinic instability problem. The dashed line is the neutral stability curve, (9.119), and the other curves are contours of growth rates obtained from (9.114). The wavenumber is scaled by $1/L_d$ (i.e., by $k_d/\sqrt{8}$) and growth rates are scaled by the inverse of the Eady time scale (i.e., by U/L_d). Thus, for $L_d = 1000\,\text{km}$ and $U = 10\,\text{m s}^{-1}$, a nondimensional growth rate of 0.25 corresponds to a dimensional growth rate of $0.25 \times 10^{-5}\,\text{s}^{-1} = 0.216\,\text{day}^{-1}$.

Note the relationship of the minimum shear to the basic state potential vorticity gradient in the respective layers. In the upper and lower layers the potential vorticity gradients are given by, respectively,

$$\frac{\partial Q_1}{\partial y} = \beta + k_d^2 U, \qquad \frac{\partial Q_2}{\partial y} = \beta - k_d^2 U. \tag{9.123a,b}$$

Thus, the requirement for instability is exactly that which causes the potential vorticity gradient to change sign somewhere in the domain, in this case becoming negative in the lower layer. This is an example of the general rule that potential vorticity (suitably generalized to include the surface boundary conditions) must change sign somewhere in order for there to be an instability.

High-wavenumber cut-off

Instability can only arise when, from (9.118),

$$4K^4(k_d^4 - K^4) > k_\beta^4 k_d^4, \tag{9.124}$$

so that a necessary condition for instability is

$$k_d^2 > K^2. \tag{9.125}$$

Thus, waves shorter than the deformation radius are always stable, no matter what the value of β. We also see from Fig. 9.14 and Fig. 9.15 that the high wavenumber cut-off in fact varies little with β if $k_d \gg k_\beta$. The critical shear required for instability approaches infinity as K approaches k_d.

Low-wavenumber cut-off

Suppose that $K \ll k_d$. Then (9.118) simplifies to $k_\beta^4 < 4K^4$. That is, for instability we require

$$K^2 > \frac{1}{2}k_\beta^2 = \frac{\beta}{2U}. \tag{9.126}$$

Thus, using (9.125) and (9.126) the unstable waves lie approximately in the interval $\beta/(\sqrt{2}U) < K < k_d$.

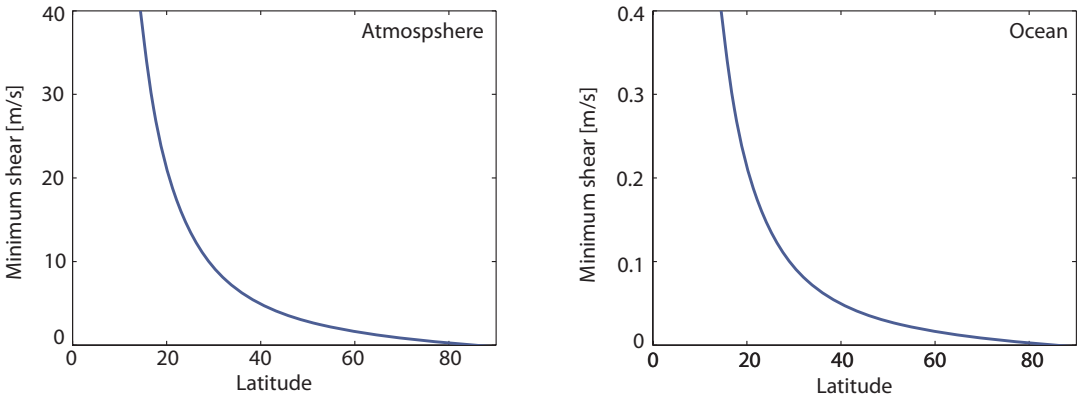

Fig. 9.16 The minimum shear (the velocity difference $U_1 - U_2$) required for baroclinic instability in a two-layer model, calculated using (9.121), i.e., $U_{min} = \beta L_d^2/4$ where $\beta = 2\Omega a^{-1}\cos\vartheta$ and $L_d = NH/f$, with $f = 2\Omega\sin\vartheta$. The left panel uses $H = 10$ km and $N = 10^{-2}\,\mathrm{s}^{-1}$, and the right panel uses parameters representative of the main thermocline, $H = 1$ km and $N = 10^{-2}\,\mathrm{s}^{-1}$. The results are not quantitatively accurate, but the implications that the minimum shear is much less for the ocean, and that in both the atmosphere and the ocean the shear increases rapidly at low latitudes, are robust.

9.7 A KINEMATIC VIEW OF BAROCLINIC INSTABILITY

In this section we take a more intuitive look at baroclinic instability, trying to understand the mechanism without treating the problem in full generality or exactness. We will do this by way of a semi-kinematic argument that shows how the waves in each layer of a two-layer model, or the waves on the top and bottom boundaries in the Eady model, can constructively interact to produce a growing instability. It is kinematic in the sense that we initially treat the waves independently, and only subsequently allow them to interact — but it is this dynamical interaction that gives the instability. We first revisit the two-layer model and simplify it to its bare essentials.

9.7.1 The Two-layer Model

A simple dynamical model

We first re-derive the instability ab initio from the equations of motion written in terms of the baroclinic streamfunction τ and the barotropic streamfunction ψ where

$$\tau \equiv \frac{1}{2}(\psi_1 - \psi_2), \qquad \psi \equiv \frac{1}{2}(\psi_1 + \psi_2). \tag{9.127}$$

We linearize about a sheared basic state of zero barotropic velocity and with $\beta = 0$. Thus, with $\psi = 0 + \psi'$ and $\tau = -Uy + \tau'$ the linearized equations of motion, equivalent to (9.107) with $\beta = 0$, are

$$\frac{\partial}{\partial t}\nabla^2\psi' = -U\frac{\partial}{\partial x}\nabla^2\tau', \tag{9.128a}$$

$$\frac{\partial}{\partial t}(\nabla^2 - k_d^2)\tau' = -U\frac{\partial}{\partial x}(\nabla^2 + k_d^2)\psi'. \tag{9.128b}$$

Neglecting the y-dependence for simplicity, we may seek solutions of the form $(\psi', \tau') = \mathrm{Re}\,(\tilde{\psi}, \tilde{\tau})\exp[\mathrm{i}k(x - ct)]$, where $c = \mathrm{i}\,c_i + c_r$, giving

$$c\tilde{\psi} - U\tilde{\tau} = 0, \tag{9.129a}$$

$$c(K^2 + k_d^2)\tilde{\tau} - U(K^2 - k_d^2)\tilde{\psi} = 0. \tag{9.129b}$$

These equations have non-trivial solutions if the determinant of the matrix of coefficients of $\tilde{\tau}$ and $\tilde{\psi}$ is zero, giving the quadratic equation $c^2(K^2 + k_d^2) - U^2(K^2 - k_d^2) = 0$. Solving this gives, reprising (9.117),

$$c = \pm U\left(\frac{K^2 - k_d^2}{K^2 + k_d^2}\right)^{1/2}. \tag{9.130}$$

Instabilities occur for $K^2 < k_d^2$, for which $c_r = 0$; that is, the wave speed is purely imaginary. From (9.129) unstable modes have

$$\tilde{\tau} = \mathrm{i}\frac{c_i}{U}\tilde{\psi} = \mathrm{e}^{\mathrm{i}\pi/2}\frac{c_i}{U}\tilde{\psi}. \tag{9.131}$$

That is, τ *lags* ψ by 90° for a growing wave ($c_i > 0$). Similarly, τ *leads* ψ by 90° for a decaying wave. Now, the temperature is proportional to τ, and in the two-level model is advected by the vertically averaged perturbation meridional velocity, v say (with Fourier amplitude $\tilde{v}$), where $v = \partial\psi/\partial x$. Thus, for growing or decaying waves,

$$\tilde{v} = \tilde{\tau}\frac{kU}{c_i}, \tag{9.132}$$

and the meridional velocity is exactly *in phase* with the temperature for growing modes, and is *out of phase* with the temperature for decaying modes. That is, for unstable modes, poleward flow is correlated with high temperatures, and for decaying modes poleward flow is correlated with low temperatures. For neutral waves, $\tilde{\tau} = c_r\tilde{\psi}/U$ and so $\tilde{v} = \mathrm{i}k\tilde{\tau}U/c_r$, and the meridional velocity and temperature are $\pi/2$ out of phase. Thus, to summarize:

- growing waves transport heat (or buoyancy) polewards;
- decaying waves transport heat equatorwards;
- neutral waves do not transport heat.

Further simplifications to the two-layer model

First consider (9.128) for waves much larger than the deformation radius, $K^2 \ll k_d^2$; we obtain

$$\frac{\partial}{\partial t}\nabla^2\psi = -U\frac{\partial}{\partial x}\nabla^2\tau, \qquad \frac{\partial}{\partial t}\tau = U\frac{\partial}{\partial x}\psi. \tag{9.133a,b}$$

for which we obtain, either directly or from (9.130), $c = \pm\mathrm{i}U$; that is, the flow is unstable. To see the mechanism, suppose that the initial perturbation is barotropic and sinusoidal in x, with no y variation. Polewards flowing fluid (i.e., $\partial\psi/\partial x > 0$) will, by (9.133b), generate a positive τ, and the baroclinic flow will be out of phase with the barotropic flow. Then, by (9.133a), the advection of τ by the mean shear produces growth of ψ that is in phase with the original disturbance. Contrast this case with that for very small disturbances, for which $K^2 \gg k_d^2$, and (9.128) becomes

$$\frac{\partial}{\partial t}\nabla^2\psi = -U\frac{\partial}{\partial x}\nabla^2\tau, \qquad \frac{\partial}{\partial t}\nabla^2\tau = -U\frac{\partial}{\partial x}\nabla^2\psi, \tag{9.134a,b}$$

or, in terms of the equations for each layer,

$$\frac{\partial}{\partial t}\nabla^2\psi_1 = -U\frac{\partial}{\partial x}\nabla^2\psi_1, \qquad \frac{\partial}{\partial t}\nabla^2\psi_2 = +U\frac{\partial}{\partial x}\nabla^2\psi_2. \tag{9.135a,b}$$

That is, the layers are completely decoupled and no instability can arise. Motivated by this, consider waves that propagate independently in each layer on the potential vorticity gradient caused by β

(if non-zero) and shear. Thus, in (9.107) we keep the potential vorticity gradients but neglect k_d^2 where it appears alongside ∇^2 and find

$$\left(\frac{\partial}{\partial t}+U\frac{\partial}{\partial x}\right)\nabla^2\psi_1'+\frac{\partial\psi_1'}{\partial x}\frac{\partial Q_1}{\partial y}=0, \tag{9.136a}$$

$$\left(\frac{\partial}{\partial t}-U\frac{\partial}{\partial x}\right)\nabla^2\psi_2'+\frac{\partial\psi_2'}{\partial x}\frac{\partial Q_2}{\partial y}=0, \tag{9.136b}$$

where $\partial Q_1/\partial y=\beta+k_d^2U$ and $\partial Q_2/\partial y=\beta-k_d^2U$. Seeking solutions of the form (9.108), the phase speeds of the associated waves are

$$c_1=U-\frac{\partial_y Q_1}{K^2},\qquad c_2=-U-\frac{\partial_y Q_2}{K^2}. \tag{9.137a,b}$$

In the upper layer the phase speed is a combination of an eastward advection and a fast westward wave propagation due to a strong potential vorticity gradient. In the lower layer the phase speed is a combination of a westward advection and a slow eastward wave propagation due to the weak potential vorticity gradient. The two phase speeds are, in general, not equal, but they would need to be so if they were to combine to cause an instability. From (9.137) this occurs when $K^2=k_d^2$ and $c_1=c_2=-\beta/k_d^2$. These conditions are just those occurring at the high-wavenumber cut-off to instability in the two-level model. At higher wavenumbers, the waves are unable to synchronize, whereas at lower wavenumbers they may become inextricably coupled.

Let us suppose that the phase of the wave in the upper layer lags (i.e., is westward of) that in the lower layer, as illustrated in the top panel Fig. 9.17. The lower panel shows the temperature field, $\tau=(\psi_1-\psi_2)/2$, and the average meridional velocity, $v=\partial_x(\psi_1+\psi_2)/2$. In this configuration, the temperature field is *in phase* with the meridional velocity, meaning that warm fluid is advected polewards. Now, let us allow the waves in the two layers to interact by adding one dynamical equation, the thermodynamic equation, which in its simplest form is

$$\frac{\partial\tau}{\partial t}=-v\frac{\partial\overline{\tau}}{\partial y}=vU, \tag{9.138}$$

where $\overline{\tau}$ is proportional to the basic state temperature field. The temperature field, τ, grows in proportion to v, which is proportional to τ if the waves tilt westwards with height, and an instability results. This dynamical mechanism is just that which is compactly described by (9.133), and an important consequence is that baroclinic waves transfer energy polewards. It is a straightforward matter to show that if the streamfunction tilts eastwards with height, v is out of phase with τ and the waves decay. A similar description applies to the Eady problem, as we now see.

9.7.2 Interacting Edge Waves in the Eady Problem

We now explore how the edge waves at the top and bottom surfaces in the Eady problem give rise to an instability, by way of a semi-kinematic description that is very similar to that of the barotropic problem described on page 343. Let us first consider the case in which the bottom and top surfaces are essentially uncoupled. Instead of solutions of (9.81) that have the structure (9.82) (which satisfies both boundary conditions), consider solutions that *separately* satisfy the bottom and top boundary conditions and that decay into the interior. These are

$$\psi_B=\mathrm{Re}\,A_B e^{ik(x-c_Tt)}e^{-\mu z/H},\qquad \psi_T=\mathrm{Re}\,A_T e^{i\phi}e^{ik(x-c_Bt)}e^{\mu(z-H)/H}, \tag{9.139a,b}$$

for the bottom and top surfaces, respectively, and ϕ is the phase shift, with A_B and A_T being real constants. The boundary conditions (9.80) then determine the phase speeds of the two systems and we find

$$c_B=\frac{\Lambda H}{\mu},\qquad c_T=\Lambda H\left(1-\frac{1}{\mu}\right). \tag{9.140a,b}$$

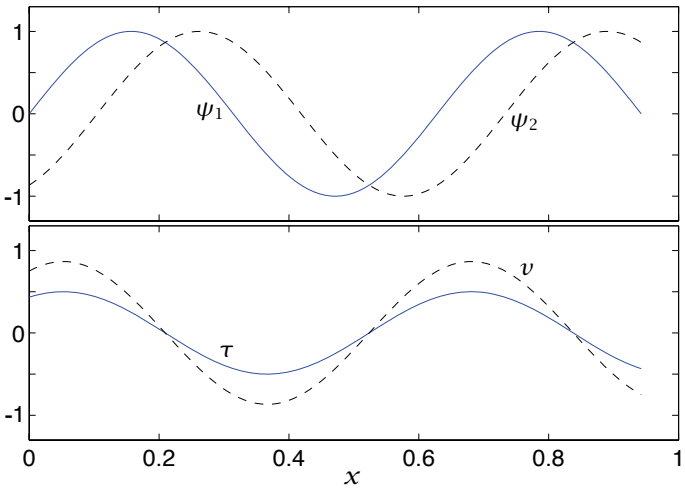

Fig. 9.17 Baroclinically unstable waves in a two layer model. The streamfunction is shown in the top panel, ψ_1 for the top layer and ψ_2 for the bottom layer. Given the westward tilt shown, the temperature, τ, and meridional velocity, v (bottom panel) are in phase, and the instability grows.

These are the phase speeds of *edge waves* in the Eady problem; they are real and in general they are unequal. It must therefore be the *interaction* of the waves on the upper and lower boundaries that is necessary for instability, because the unstable wave has but a single phase speed. This interaction can occur when their phase speeds are equal, and from (9.140) this occurs when $\mu = 2$, giving

$$k = \frac{2}{L_d} \qquad \text{and} \qquad c = \frac{\Lambda H}{2}. \tag{9.141a,b}$$

This phase speed is just that of the flow at mid-level, and at the critical wavenumber in the full Eady problem, $k_c = 2.4/L_d$, from (9.90), the phase speed is purely real and equal to that of (9.141b) — see Fig. 9.10. Thus, (9.141) approximately characterizes the critical wavenumber in the full problem.

To turn this kinematic description into a dynamical instability, suppose that the two rigid surfaces are close enough so that the waves can interact, but still far enough so that their structure is approximately given by (9.139). (Note that if μ is too large, the waves decay rapidly away from the edges and will not intersect.) Specifically, let the buoyancy perturbation at a given boundary be advected by the total meridional velocity perturbation, including that arising from the perturbation at the other boundary, so that at the top and bottom boundaries

$$\frac{\partial b'_T}{\partial t} = -(v'_B + v'_T)\frac{\partial \bar{b}_T}{\partial y}, \qquad \frac{\partial b'_B}{\partial t} = -(v'_B + v'_T)\frac{\partial \bar{b}_B}{\partial y}. \tag{9.142}$$

The waves will reinforce each other if v'_T is in phase with b'_B at the lower boundary, and if v'_B is in phase with b'_T at the upper boundary. Now, using (9.139), the velocity and buoyancy associated with the edge waves are given by

$$b_B = -\text{Re } kNA_B e^{-\mu z/H} e^{ikx}, \qquad b_T = \text{Re } kNA_T e^{i\phi} e^{\mu(z-H)/H} e^{ikx}, \tag{9.143a}$$

$$v_B = \text{Re } ikA_B e^{-\mu z/H} e^{ikx}, \qquad v_T = \text{Re } ikA_T e^{i\phi} e^{\mu(z-H)/H} e^{ikx}. \tag{9.143b}$$

The fields b_B and v_T, and b_T and v_B, will be positively correlated if $0 < \phi < \pi$, and will be exactly in phase if $\phi = \pi/2$, and this case is illustrated in Fig. 9.18. Just as in the two-layer case, this phase corresponds to a westward tilt with height, and it is this, in conjunction with geostrophic and hydrostatic balance, that allows warm fluid to move polewards and available potential energy to be released. From (9.142), the perturbation will grow and an instability will result. The analogy between baroclinic instability and barotropic instability should be evident from the similarity of this description and that of Section 9.2.4, with z in the baroclinic problem playing the role of y in

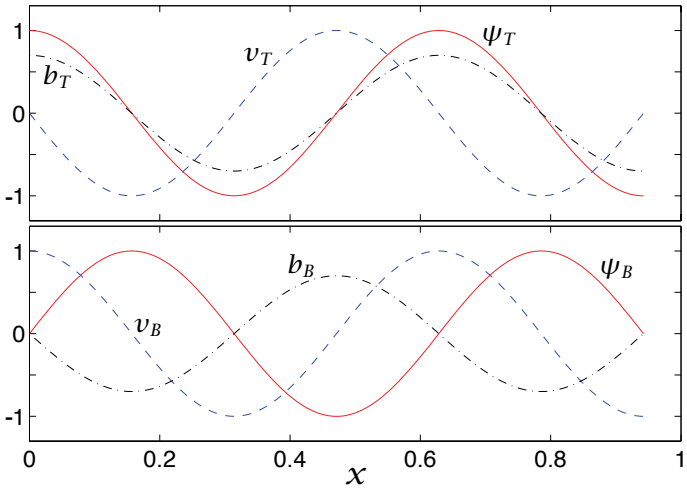

Fig. 9.18 Interacting edge waves in the Eady model. The upper panel shows waves on the top surface, and the lower panel shows waves on the bottom. If the streamfunction tilts westwards with height, then the temperature on the top (bottom) is correlated with the meridional velocity on the bottom (top), the waves can reinforce each other. See also Fig. 9.12.

the barotropic problem, and b the role of u; note that (9.142) is almost identical to (9.45). However, the analogy of the two problems in full is not perfect because the boundary condition that $w = 0$ does not have an exact correspondence in the barotropic problem. More importantly, the nonlinear development of the baroclinic problem, discussed in Chapter 12, is generally three-dimensional, which need not be the case in the barotropic problem.

9.8 ♦ THE ENERGETICS OF LINEAR BAROCLINIC INSTABILITY

In baroclinic instability, warm parcels move polewards and cold parcels move equatorwards. This motion draws on the available potential energy of the mean state, because warm light parcels move upwards and cold dense parcels move downwards and the height of the mean centre of gravity of the fluid falls, and the loss of potential energy is converted to kinetic energy of the perturbation. However, because the instability is growing, the energy of the perturbation is of course not conserved, and both the kinetic energy and the available potential energy of the perturbation will grow. However, we still expect a conversion of potential energy to kinetic energy, and the purpose of this section is to demonstrate that explicitly. For simplicity, we restrict attention to the flat-bottomed two-level model with $\beta = 0$.

As in Section 5.6, the energy may be partitioned into kinetic energy and available potential energy. In a three-dimensional quasi-geostrophic flow the kinetic energy is given by, in general,

$$\mathrm{KE} = \frac{1}{2}\int (\nabla\psi)^2 \,\mathrm{d}V, \tag{9.144}$$

which, in the case of the two-layer model becomes

$$\mathrm{KE} = \frac{1}{2}\int (\nabla\psi_1)^2 + (\nabla\psi_2)^2 \,\mathrm{d}A = \int (\nabla\psi)^2 + (\nabla\tau)^2 \,\mathrm{d}A. \tag{9.145}$$

Restricting attention to a single Fourier mode this becomes

$$\mathrm{KE} = k^2\tilde{\psi}^2 + k^2\tilde{\tau}^2. \tag{9.146}$$

The available potential energy in the continuous case is given by

$$\mathrm{APE} = \frac{1}{2}\int \left(\frac{f_0}{N}\right)^2 \left(\frac{\partial\psi}{\partial z}\right)^2 \mathrm{d}V. \tag{9.147}$$

For a single Fourier mode in a two-layer model this becomes

$$\text{APE} = k_d^2 \tilde{\tau}^2. \tag{9.148}$$

Now, the nonlinear vorticity equations for each level are

$$\frac{\partial}{\partial t}\nabla^2\psi_1 + J(\psi_1, \nabla^2\psi_1) = -2\frac{f_0 w}{H}, \tag{9.149a}$$

$$\frac{\partial}{\partial t}\nabla^2\psi_2 + J(\psi_2, \nabla^2\psi_2) = 2\frac{f_0 w}{H}, \tag{9.149b}$$

where w is the vertical velocity between the levels. (These equations are the two-level analogues of the continuous vorticity equation, with the right-hand sides being finite-difference versions of $f_0 \partial w/\partial z$.) Multiplying the two equations of (9.149) by $-\psi_1$ and $-\psi_2$, respectively, and adding we readily find

$$\frac{\mathrm{d}}{\mathrm{d}t}\text{KE} = \frac{4f_0}{H}\int w\tau \,\mathrm{d}A. \tag{9.150a}$$

For a single Fourier mode this becomes

$$\frac{\mathrm{d}}{\mathrm{d}t}\text{KE} = \text{Re}\,\frac{4f_0}{H}\tilde{w}\tilde{\tau}^*, \tag{9.150b}$$

where $w = \tilde{w}\exp[\mathrm{i}(kx - ct)] + \text{c.c.}$, and the asterisk denotes a complex conjugate.

The continuous thermodynamic equation is

$$\frac{\mathrm{D}b}{\mathrm{D}t} + wN^2 = 0. \tag{9.151}$$

Using $b = f_0 \partial\psi/\partial z$ and finite-differencing (with $\partial\psi/\partial z \to (\psi_1 - \psi_2)/(H/2) = 4\tau/H$), we obtain the two-level thermodynamic equation:

$$\frac{\partial\tau}{\partial t} + J(\psi, \tau) + \frac{wN^2 H}{4f_0} = 0. \tag{9.152}$$

The change of available potential energy is obtained from this by multiplying by $k_d^2\tau$ and integrating, giving

$$\int\left(\frac{1}{2}\frac{\mathrm{d}}{\mathrm{d}t}k_d^2\tau^2 + \tau w\frac{2f_0}{H}\right)\mathrm{d}A = 0, \tag{9.153}$$

or

$$\frac{\mathrm{d}}{\mathrm{d}t}\text{APE} = -\frac{4f_0}{H}\int w\tau \,\mathrm{d}A, \tag{9.154a}$$

or, for a single Fourier mode,

$$\frac{\mathrm{d}}{\mathrm{d}t}\text{APE} = -\text{Re}\,\frac{4f_0}{H}\tilde{w}\,\tilde{\tau}^*. \tag{9.154b}$$

From (9.150) and (9.154) it is clear that in the nonlinear equations the sum of the kinetic energy and the available potential energy is conserved.

We now specialize by obtaining w from the linear baroclinic instability problem. Using this in (9.150) and (9.154) will give us the conversion between kinetic energy and potential energy in the growing baroclinic wave. It is important to realize that the total energy of the disturbance will not be conserved — both the potential and kinetic energy are growing, exponentially in this problem, because they are extracting energy from the mean state. To calculate w we use the linearized thermodynamic equation. From (9.152) this is

$$\frac{\partial\tau}{\partial t} - U\frac{\partial\psi}{\partial x} + \frac{HwN^2}{4f_0} = 0, \tag{9.155}$$

omitting the primes on perturbation quantities. For a single Fourier mode, this gives

$$\frac{HN^2}{4f_0}\tilde{w} = \mathrm{i}k(c\tilde{\tau} + U\tilde{\psi}). \tag{9.156}$$

But, from (9.129), $c\tilde{\psi} = U\tilde{\tau}$ in two-layer f-plane baroclinic instability and so

$$\frac{HN^2}{4f_0}\tilde{w} = \mathrm{i}kc\tilde{\tau}\left(1 + \frac{U^2}{c^2}\right) = \mathrm{i}kc\tilde{\tau}\left(\frac{2K^2}{K^2 - k_d^2}\right), \tag{9.157}$$

using (9.130). For stable waves, $K^2 > k_d^2$ and $c = c_r$ and in that case the vertical velocity is $\pi/2$ out of phase with the temperature, and there is no conversion of APE to KE. For unstable waves $c = \mathrm{i}\,c_i$ and $K^2 < k_d^2$, and the vertical velocity is in phase with the temperature; that is, *warm air is rising and there is a conversion of APE to KE*. To see this more formally, recall that the conversion from APE to KE is given by $4\tilde{w}\tilde{\tau}^* f_0/H$. Thus, using (9.157),

$$\frac{\mathrm{d}}{\mathrm{d}t}(\mathrm{APE} \to \mathrm{KE}) = \mathrm{Re}\, 2\mathrm{i}kck_d^2\left(\frac{2K^2}{K^2 - k_d^2}\right)\tilde{\tau}^2, \tag{9.158}$$

using also the definition of k_d given in (9.103). If the wave is growing, then $K^2 < k_d^2$ and $c = \mathrm{i}c_i$ and the right-hand side is real and positive. For neutral waves, if $c = c_r$ the right-hand side of (9.158) is pure imaginary, and so the conversion is zero. This completes our demonstration that baroclinic instability converts potential energy into kinetic energy.

9.9 ✦ BETA, SHEAR AND STRATIFICATION IN A CONTINUOUS MODEL

The two-layer model of Section 9.6 indicates that β has a number of important effects on baroclinic instability. Do these carry over to the continuously stratified case? The answer by and large is yes, but with some important qualifications that generally concern weak or shallow instabilities. In particular, we will find that there is no short-wave cut-off in the continuous model with non-zero beta, and that the instability determines its own depth scale. We will illustrate these properties first by way of scaling arguments and then by way of numerical calculations.[13]

9.9.1 Scaling Arguments and Estimates

With finite density scale height and non-zero β, the quasi-geostrophic potential vorticity equation, linearized about a mean zonal velocity $U(z)$, is

$$\left(\frac{\partial}{\partial t} + U\frac{\partial}{\partial x}\right)q' + \frac{\partial\psi'}{\partial x}\frac{\partial Q}{\partial y} = 0, \tag{9.159}$$

where

$$q' = \nabla^2\psi' + \frac{f_0^2}{\rho_R}\frac{\partial}{\partial z}\left(\frac{\rho_R}{N^2}\frac{\partial\psi'}{\partial z}\right), \qquad \frac{\partial Q}{\partial y} = \beta - \frac{f_0^2}{\rho_R}\frac{\partial}{\partial z}\left(\frac{\rho_R}{N^2}\frac{\partial U}{\partial z}\right), \tag{9.160a,b}$$

and ρ_R is a specified density profile. If we assume that $U = \Lambda z$ where Λ is constant and that N is constant, and let $H_\rho^{-1} = -\rho_R^{-1}\partial\rho_R/\partial z$, then

$$\frac{\partial Q}{\partial y} = \beta + \frac{f_0^2\Lambda}{N^2 H_\rho} = \beta(1 + \alpha), \quad \text{where} \quad \alpha = \left(\frac{f_0^2\Lambda}{\beta N^2 H_\rho}\right). \tag{9.161}$$

The boundary conditions on (9.159) are

$$\left(\frac{\partial}{\partial t}+U\frac{\partial}{\partial x}\right)\frac{\partial\psi'}{\partial z}-\frac{\partial\psi'}{\partial x}\frac{\partial U}{\partial z}=0, \qquad \text{at } z=0, \tag{9.162}$$

and that $\psi \to 0$ as $z \to \infty$. The problem we have defined essentially constitutes the Charney problem. We can reduce this to the Eady problem by setting $\beta = 0$ and $H_\rho = \infty$, and providing a lid that is some finite height above the ground.

As in the Eady problem, we seek solutions of the form

$$\psi = \mathrm{Re}\,\tilde{\psi}(z)\mathrm{e}^{\mathrm{i}(kx+ly-kct)}, \tag{9.163}$$

and substituting into (9.159) gives

$$\left(\frac{f_0^2}{H_\rho^2N^2}\right)\left(H_\rho^2\frac{\mathrm{d}^2\tilde{\psi}}{\mathrm{d}z^2}-H_\rho\frac{\mathrm{d}\tilde{\psi}}{\mathrm{d}z}\right)-\left(K^2-\frac{\beta+\Lambda f_0^2/(N^2H_\rho)}{\Lambda z-c}\right)\tilde{\psi}=0. \tag{9.164}$$

The Boussinesq version of this expression, for a fluid contained between two horizontal surfaces, is obtained by letting $H_\rho = \infty$, giving

$$\left(\frac{f_0^2}{N^2}\right)\frac{\mathrm{d}^2\tilde{\psi}}{\mathrm{d}z^2}-\left(K^2-\frac{\beta}{\Lambda z-c}\right)\tilde{\psi}=0. \tag{9.165}$$

It seems natural to nondimensionalize (9.164) using:

$$z=H_\rho\hat{z}, \qquad c=\Lambda H_\rho\hat{c}, \qquad K=\left(\frac{f_0}{NH_\rho}\right)\widehat{K}, \tag{9.166}$$

whence the equation becomes

$$\frac{\mathrm{d}^2\tilde{\psi}}{\mathrm{d}\hat{z}^2}-\frac{\mathrm{d}\tilde{\psi}}{\mathrm{d}\hat{z}}-\left(\widehat{K}^2-\frac{\gamma+1}{\hat{z}-\hat{c}}\right)\tilde{\psi}=0, \tag{9.167}$$

where

$$\gamma=\alpha^{-1}=\frac{\beta N^2H_\rho}{f_0^2\Lambda}=\frac{\beta L_d^2}{H_\rho\Lambda}=\frac{H_\rho}{h}, \tag{9.168}$$

where $h \equiv \Lambda f_0^2/(\beta N^2)$. The nondimensional parameter γ is known as the Charney–Green number.[14] The Boussinesq version, (9.165), may be nondimensionalized using H_D in place of H_ρ, where H_D is the depth of the fluid between two rigid surfaces. In that case

$$\frac{\mathrm{d}^2\tilde{\psi}}{\mathrm{d}\hat{z}^2}-\left(\widehat{K}^2-\frac{\gamma}{\hat{z}-\hat{c}}\right)\tilde{\psi}=0, \tag{9.169}$$

where here the nondimensional variables are scaled with H_D.

Now, suppose that γ is large, for example if β or the static stability are large or the shear is weak. Equation (9.167) admits no non-trivial balance, suggesting that we rescale the variables using h instead of H_ρ as the vertical scale in (9.166). The rescaled version of (9.167) is then

$$\frac{\mathrm{d}^2\tilde{\psi}}{\mathrm{d}\hat{z}^2}-\frac{1}{\gamma}\frac{\mathrm{d}\tilde{\psi}}{\mathrm{d}\hat{z}}-\left(\widehat{K}^2-\frac{1+\gamma^{-1}}{\hat{z}-\hat{c}}\right)\tilde{\psi}=0, \tag{9.170}$$

or, approximately,

$$\frac{\mathrm{d}^2\tilde{\psi}}{\mathrm{d}\hat{z}^2}-\left(\widehat{K}^2-\frac{1}{\hat{z}-\hat{c}}\right)\tilde{\psi}=0. \tag{9.171}$$

This is exactly the same equation as results from a similar rescaling of the Boussinesq system, (9.169), as we might have expected because now the dynamical vertical scale, h, is much smaller than the scale height H_ρ (or H_D) and the system is essentially Boussinesq. Thus, noting that (9.171) has the same nondimensional form as (9.169) save that γ is replaced by unity, and that (9.171) with $\gamma = 1$ must produce the same scales and growth rates as in the Eady problem, we may deduce that:

(i) the wavelength of the instability is $\mathcal{O}(Nh/f_0)$;

(ii) the growth rate of the instability is $\mathcal{O}(Kc) = \mathcal{O}(f_0\Lambda/N)$;

(iii) the vertical scale of the instability is $\mathcal{O}(h) = \mathcal{O}(f_0^2\Lambda/(\beta N^2))$.

These are the same as for the Eady problem, except with the dynamical height h replacing the geometric or scale height H_D. Effectively, the dynamics has determined its own vertical scale, h, which is much less than the scale height or geometric height, producing 'shallow modes'.

In the limit $\gamma \ll 1$ (strong shear, weak β), the Boussinesq and compressible problems differ. The Boussinesq problem reduces to the Eady problem, considered previously, whereas (9.167) becomes, approximately,

$$\frac{\mathrm{d}^2\tilde{\psi}}{\mathrm{d}\tilde{z}^2} - \frac{\mathrm{d}\tilde{\psi}}{\mathrm{d}\tilde{z}} - \left(\widehat{K}^2 - \frac{1}{\tilde{z} - \hat{c}}\right)\tilde{\psi} = 0, \tag{9.172}$$

and in this limit the appropriate vertical scale is the density scale height H_ρ. Because $H_\rho \gg h$ these are 'deep modes', occupying the entire vertical extent of the domain.

The scale h does not arise in the two-level model, but there is a connection between it and the critical shear for instability in the two-level model. The condition $\gamma \ll 1$, or $h \gg H$, may be written as

$$H\Lambda \gg \beta\left(\frac{NH}{f_0}\right)^2. \tag{9.173}$$

Compare this with the necessary condition for instability in a two-level model, (9.122), namely

$$(U_1 - U_2) > \beta\left(\frac{NH_\Delta}{f_0}\right)^2, \tag{9.174}$$

where H_Δ is the vertical distance between the two levels. Thus, essentially the same condition governs the onset of instability in the two-level model as governs the production of deep modes in the continuous model. This correspondence is a natural one, because in the two-level model *all* modes are 'deep', and the model fails (as it should) to capture the shallow modes of the continuous system. For similar reasons, there is a high-wavenumber cut-off in the two-level model: in the continuous model these modes are shallow and so cannot be captured by two-level dynamics. Somewhat counter-intuitively, for these modes the β-effect must be important, even though the modes have small horizontal scale: when $\beta = 0$ the instability arises via an interaction between edge waves at the top and bottom of the domain, whereas the shallow instability arises via an interaction of the edge waves at the surface with Rossby waves just above the surface.

9.9.2 Some Numerical Calculations

Adding β to the Eady model

Our first step is to add the β-effect to the Eady problem.[15] That is, we suppose a Boussinesq fluid with uniform stratification, that the shear is zonal and constant and that the entire problem is sandwiched between two rigid surfaces. Growth rates and phase speeds of such an instability calculation are illustrated in Fig. 9.19 and the vertical structure is shown in Fig. 9.20. As in the two-layer problem, there is a low-wavenumber cut-off to the main instability, although there is now an additional weak instability at very large-scales. These so-called *Green modes* have no counterpart in the two-layer model — they are deep, slowly growing modes that will be dominated by faster growing

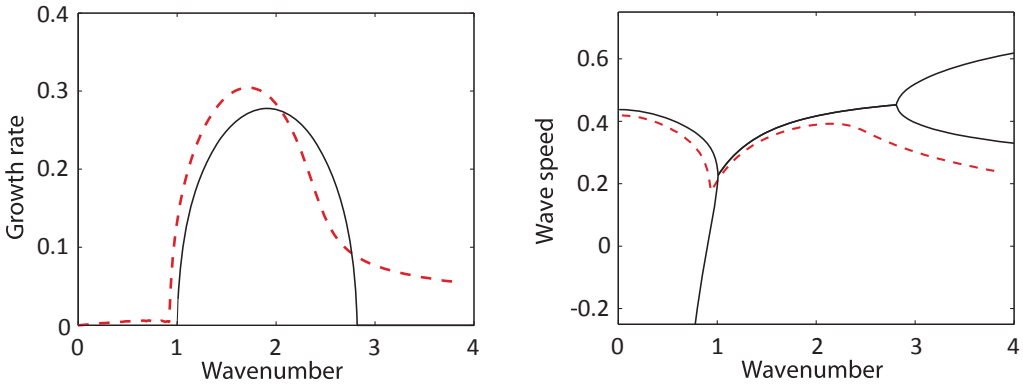

Fig. 9.19 Growth rates and wave speeds for the two-layer (solid) and continuous (dashed) models, with the same values of the Charney–Green number, γ, and uniform shear and stratification. (In the two-layer case $\gamma = \beta L_d^2/[2(U_1 - U_2)] = 0.5$, and in the continuous case $\gamma = \beta L_d^2/(H\Lambda) = 0.5$.) In the continuous case only the wave speed associated with the unstable mode is shown. In the two-layer case there are two real wave speeds which coalesce in the unstable region.

modes in most real situations. (Also, the fact that the Green modes have a scale much larger than the deformation scale suggests a degree of caution in the accuracy of the quasi-geostrophic calculation.) At high wavenumbers there is no cut-off to the instability in the continuous problem in the case of non-zero beta; the high-wavenumber modes are shallow and unstable via an interaction between edge waves at the lower boundary and Rossby waves in the lower atmosphere, and so have no counterpart in either the two-layer problem (where the modes are deep) or the Eady problem (which has no Rossby waves).

Effects of non-uniform shear and stratification

If the shear or stratification is non-uniform an analytic treatment is, even in problems without β, usually impossible and the resulting equations must be solved numerically. However, if we restrict attention to a *discontinuity* in the shear or the stratification, then the resulting problem is very similar to the problem with rigid boundaries, and this property provides some justification for using the Eady problem to model instabilities in the Earth's atmosphere: in the troposphere the stratification is (approximately) constant, and the rapid increase in stratification in the stratosphere can be approximated by a lid at the tropopause. Heuristically, we can see this from the form of the thermodynamic equation, namely

$$\frac{\mathrm{D}b}{\mathrm{D}t} + N^2 w = 0. \tag{9.175}$$

If N^2 is high this suggests w will be small, and a lid is the limiting case of this. The oceanic problem is rather more involved, because although both the stratification and the shear are concentrated in the upper ocean, they vary relatively smoothly; furthermore, the shear is high where the stratification is high, and the two have opposing effects.

To go one step further, consider the Boussinesq potential vorticity equation, linearized about a zonally uniform state $\Psi(y, z)$, with a rigid surface at $z = 0$. The normal-mode evolution equations are similar to (9.69), namely

$$(U - c)\left[\frac{\partial^2}{\partial y^2} - k^2 + \frac{\partial}{\partial z}\left(F\frac{\partial}{\partial z}\right)\right]\widetilde{\psi} + \frac{\partial Q}{\partial y}\widetilde{\psi} = 0, \qquad z > 0, \tag{9.176a}$$

$$(U - c)\frac{\partial \widetilde{\psi}}{\partial z} - \frac{\partial U}{\partial z}\widetilde{\psi} = 0, \qquad \text{at } z = 0, \tag{9.176b}$$

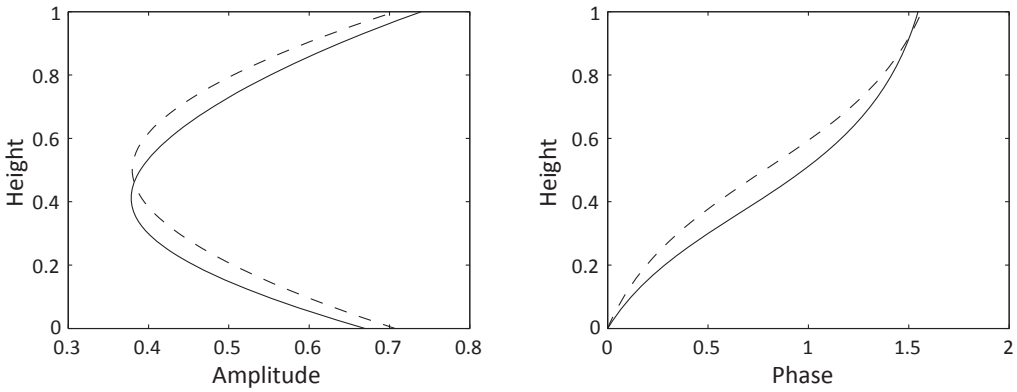

Fig. 9.20 Vertical structure of the most unstable modes in a continuously stratified instability calculation with $\beta = 0$ (dashed lines, the Eady problem) and $\beta \neq 0$ (solid lines, as in the continuous problem in Fig. 9.19). The effect of beta is to depress the height of the maximum amplitude of the instability.

where $\partial_y Q = \beta - \partial_{yy} U - \partial_z (F \partial_z U)$. Now suppose that there is a discontinuity in the shear and/or the stratification in the interior of the fluid, at some level $z = z_c$. Integrating (9.176a) across the discontinuity, noting that $\widetilde{\psi}$ is continuous in z, gives

$$(U - c) \left[F \frac{\partial \widetilde{\psi}}{\partial z} \right]_{z_c-}^{z_c+} - \widetilde{\psi}(y, z_c) \left[F \frac{\partial U}{\partial z} \right]_{z_c-}^{z_c+} = 0. \tag{9.177}$$

which has similar form to (9.176b). This construction is evocative of the equivalence of a delta-function sheet of potential vorticity at a rigid boundary, except that now a discontinuity in the potential vorticity in the *interior* has a similarity with a rigid boundary.

We can illustrate the effects of an interior discontinuity that crudely represents the tropopause by numerically solving the linear eigenvalue problem. We pose the problem on the f-plane, in a horizontally doubly-periodic domain, with no horizontal variation of shear, and between two horizontal rigid lids. The eigenvalue problem is defined by (9.69), and the numerical procedure then solves for the complex eigenvalue c and eigenfunction $\widetilde{\psi}(z)$; various results are illustrated in Fig. 9.21. To parse this rather complex figure, first look at the solid curves in all the panels. These arise when the problem is solved with a uniform shear and a uniform stratification, with a lid at $z = 0$ and $z = 1$, hence simply giving the Eady problem. The familiar growth rates and vertical structure of the solution are given by the solid curves in panels (b), (c) and (d), and these are just the same as in Fig. 9.10. The various dotted and dashed curves show the results when the lid at $z = 1$ is replaced by a stratosphere stretching from $1 < z < 2$ either with high stratification, zero shear, or both, and in all of these cases the stratosphere acts qualitatively in the same way as a rigid lid. The vertical structure of the solution in the troposphere is, in all cases, quite similar, and the amplitude decays rapidly above the idealized tropopause, consistent with the almost uniform phase of the disturbance illustrated in panel (d) — recall that a tilting of the disturbance with height is necessary for instability. It is these properties that make the Eady problem of more general applicability to the Earth's atmosphere than might be first thought: the high stratification above the tropopause and consequent decay of the instability are mimicked by the imposition of a rigid lid.

In the ocean, the stratification is highest in its upper regions (e.g., in the main thermocline) where the shear is also strongest, and numerical calculations of the structure and growth rate of idealized profiles are illustrated in Fig. 9.22.[16] The solid curve shows the Eady problem, and the various dashed curves show the phase speeds, growth rates and phase with combinations of the profiles illustrated in panel (a). Much of the ocean is characterized by having both a higher shear

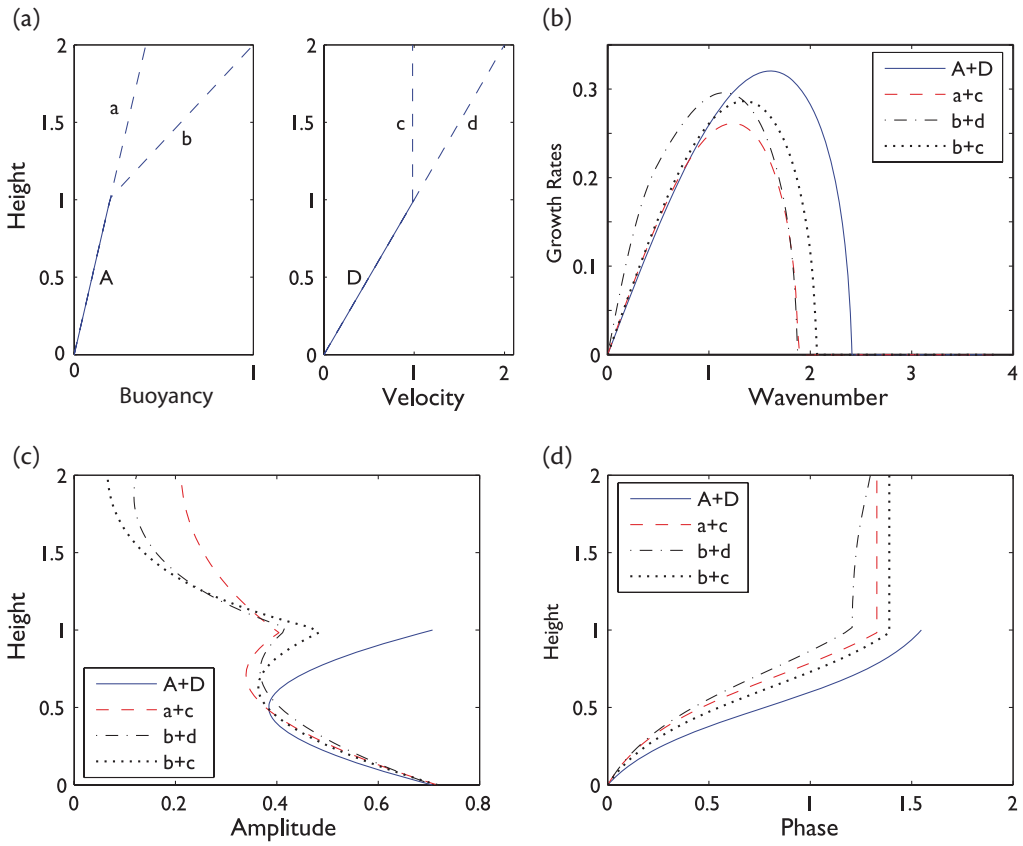

Fig. 9.21 The effect of a stratosphere on baroclinic instability: (a) the given profiles of shear and stratification; (b) the growth rate of the instabilities; (c) the amplitude of the most unstable mode as a function of height; (d) the phase of the most unstable mode. The instability problem is solved numerically with various profiles of stratification and shear. In each profile, in the idealized troposphere ($z < 1$) the shear and stratification are uniform and the same in each case. We consider four idealized stratospheres ($z \geq 1$): (1) A lid at $z = 1$, i.e., no stratosphere, giving the Eady problem itself (profiles A+D, solid lines); (2) stratospheric stratification as for the troposphere, but with zero shear (profiles a+c, dashed); (3) stratospheric shear as for troposphere, but with stratification (N^2) four times the tropospheric value (b+d, dot-dashed); (4) zero shear and high stratification in the stratosphere (b+c, dotted). In the troposphere the amplitude and structure of the instability are similar in all cases, illustrating the similarity of a rigid lid and abrupt changes in shear or stratification. Either a high stratification or a low shear (or both) will result in weak stratospheric instability.

and a higher stratification in the upper 1 km or so, and this case is shown with the dotted line in Fig. 9.22. The amplitude of the instability is also largely confined to the upper ocean, and unlike the Eady problem it does not arise through the interaction of edge waves at the top and bottom: the potential vorticity changes sign because of the interior variations due to the non-uniform shear, mainly in the upper ocean. Consistently, the phase of the baroclinic waves is nearly constant in the lower ocean in those cases in which the shear is confined to the upper ocean. The real ocean is still more complicated, because the most unstable regions near intense western boundary currents are often also barotropically unstable, and the mean flow itself may be meridionally directed. Nevertheless, the result that linear baroclinic instability is primarily an *upper ocean* phenomenon is quite robust. However, we will find in Chapter 12 that the nonlinear evolution of baroclinic instability leads to eddies throughout the water column.

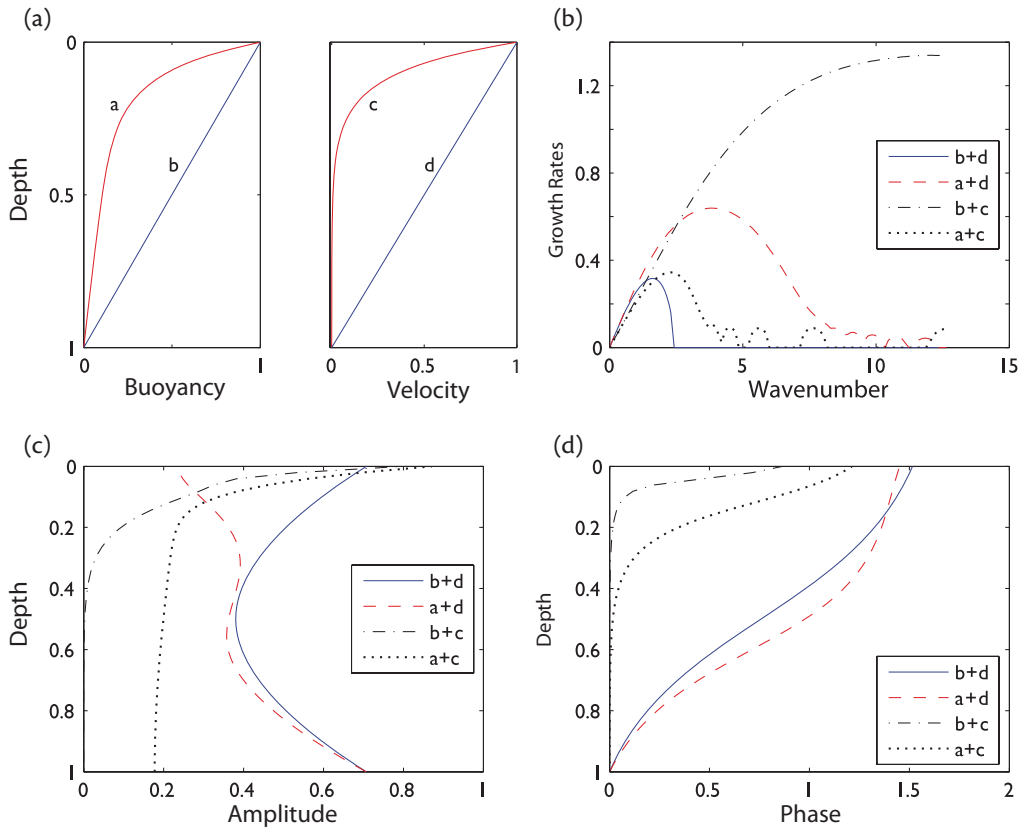

Fig. 9.22 The baroclinic instability in an idealized ocean, with four different profiles of shear or stratification. The panels are: (a) the profiles of velocity and buoyancy (and so N^2) used; (b) the growth rates of the various cases; (c) the vertical structure of the amplitude of the most unstable models; (d) the phase in the vertical of the most unstable modes. The instability is calculated numerically with four combinations of shear and stratification: (1) uniform stratification and shear i.e., the Eady problem, (profiles b+d, solid lines); (2) uniform shear, upper-ocean enhanced stratification (a+d, dashed); (3) uniform stratification, upper ocean enhanced shear (b+c, dot-dashed); (4) both stratification and shear enhanced in the upper ocean (a+c, dotted). Case 2 (a+d, dashed) is really more like an atmosphere with a stratosphere (see Fig. 9.21), and the amplitude of the disturbance falls off, rather unrealistically, in the upper ocean. Case 4 (a+c, dotted) is the most oceanographically relevant.

Notes

1 Thomson (1871), Helmholtz (1868). Thomson later became known as Lord Kelvin.

2 This is Squire's theorem, which states that for every three-dimensional disturbance to a plane-parallel flow there exists a more unstable two-dimensional one (Squire 1933). This means there is no need to consider three-dimensional effects to determine whether such a flow is unstable.

3 Rayleigh (1880). John Strutt (1842–1919) became 3rd Baron Rayleigh on the death of his father in 1873 and, in a testament to the enduring British class system, is almost universally known as Lord Rayleigh. He made major contributions in many areas of physics, among them fluid mechanics (including the theory of sound and instability theory), the analysis of the composition of gases (leading to the discovery of argon), and scattering theory.

4 First obtained by Rayleigh (1894). I thank Adrian Matthews for comments and pointing out an error in an earlier derivation. For more applications of this kind of argument see Harnik & Heifetz (2007) and references therein.

5 Rayleigh (1880) and, for the case with β, Kuo (1949).

6 Fjørtoft (1950).

7 Charney & Stern (1962), Pedlosky (1964).

8 Eady (1949), Charney (1947). Eric Eady (1915–1966) is best remembered today as the author of the iconic 'Eady model' of baroclinic instability, which describes the fundamental hydrodynamic instability mechanism that gives rise to weather systems. After an undergraduate education in mathematics he joined the UK Meteorological Office in 1937, becoming a forecaster and upper air analyst, in which capacity he served throughout the war. In 1946 he joined the Department of Mathematics at Imperial College, presenting his PhD thesis in 1948 on 'The theory of development in dynamical meteorology', subsequently summarized in *Tellus* (Eady 1949). This work, with a skilled combination of austerity and relevance, provides a mathematical description of the essential aspects of cyclone development that stands to this day as a canonical model in the field. It also includes, rather obliquely, a derivation of the stratified quasi-geostrophic equations, albeit in a special form. The impact of the work was immediate and it led to visits to Bergen (in 1947 with J. Bjerknes), Stockholm (in 1952 with C.-G. Rossby) and Princeton (in 1953 with J. von Neumann and Charney). Eady followed his baroclinic instability work with prescient discussions of the general circulation of the atmosphere (Eady 1950, Eady & Sawyer 1951, Eady 1954). A perfectionist who sought to understand it all, Eady's subsequent published output was small and he later turned his attention to fundamental problems in other areas of fluid mechanics, the dynamics of the Sun and the Earth's interior, and biochemistry. In his younger days he was a lively personality but he became increasingly divorced from normal scientific and human discourse, and finally took his own life. There is little published about him, save for the obituary by Charnock *et al.* (1966). Elsewhere, Charnock said 'Talking with Eric Eady was one of the pleasures of life'.

Jule Charney (1917–1981) played a defining role in dynamical meteorology in the second half of the twentieth century. He made seminal contributions in many areas including: the theory of baroclinic instability (Charney 1947); a systematic scaling theory for large-scale atmospheric motions and the derivation of the quasi-geostrophic equations (Charney 1948); a theory of stationary waves in the atmosphere (Charney & Eliassen 1949); the demonstration of the feasibility of numerical weather forecasts (Charney *et al.* 1950); planetary wave propagation into the stratosphere (Charney & Drazin 1961); a criterion for baroclinic instability (Charney & Stern 1962); a theory for hurricane growth (Charney & Eliassen 1964); and the concept of geostrophic turbulence (Charney 1971). His PhD from UCLA in 1946 was entitled 'Dynamics of long waves in a baroclinic westerly current' and this became his well-known 1947 paper. After this he spent a year at Chicago and another at Oslo, and in 1948 joined the Institute of Advanced Study in Princeton where he stayed until 1956 (and where Eady visited for a while). He spent most of his subsequent career at MIT, interspersed with many visits to Europe, especially Norway. For a more complete picture of Charney, see Lindzen *et al.* (1990) and a brief biography by N. Phillips, available at http://www.nap.edu/readingroom/books/biomems/jcharney.html.

9 The solution to Eady problem follows relatively straightforwardly using the quasi-geostrophic approximation from the outset. But when Eady was formulating his problem the quasi-geostrophic equations were not known, except perhaps to Charney. Eady (1949) began with something more akin to the primitive equations, and introduced an essentially quasi-geostrophic assumption late in his derivation, and independently derived a linear version of the quasi-geostrophic potential vorticity equation.

10 If c is real (and the waves are neutral), then there exists the possibility that $\Lambda z - c = 0$, and the equation for Φ is

$$\frac{\mathrm{d}^2\Phi}{\mathrm{d}z^2} - \mu^2\Phi = C\delta(z - z_c), \qquad z_c = c/\Lambda, \tag{9.178}$$

where C is a constant. Because z_c is continuous in the interval $[0, 1]$ so is c, and these solutions have a continuous spectrum of eigenvalues. The associated eigenfunctions provide formal completeness to the normal modes, enabling any function to be represented as their superposition.

11 After Phillips (1954).

12 Our nondimensionalization of the two-layer system is such as to be in correspondence with that for the continuous system. Thus we choose H to be the total depth of the domain. This choice produces growth rates and wavenumbers that are equivalent to those in the Eady problem.

13 Green (1960) and Branscome (1983). Lindzen & Farrell (1980) also provide an approximate calculation of growth rates in the Charney problem.

14 After Charney (1947), in whose problem it appears, and Green (1960), who appreciated its importance.

15 Our numerical procedure is to assume a wave-like solution in the horizontal direction of the form $\tilde{\psi}\exp[\mathrm{i}(kx + ly - \omega t)]$, and to finite difference the equations in the vertical direction. The resulting eigenvalue equations are solved by standard matrix methods, for each horizontal wavenumber. See Smith & Vallis (1998) and Green (1960).

16 Gill *et al.* (1974) and Robinson & McWilliams (1974) were among the first to look at baroclinic instability in the ocean.